

Daniel Blanco Garde

CORRESPONDENCE BETWEEN ADHESIVE JOINT STRENGTH, SURFACE TREATMENT AND SURFACE QUALITY OF CFRP

Master's Thesis
Faculty of Engineering and
Natural Sciences
D. Sc. Jarno Jokinen
D. Sc. Farzin Javanshour
June 2023

ABSTRACT

Daniel Blanco Garde: Correspondence between adhesive joint strength, surface treatment and surface quality of CFRP

Master's Degree

Tampere University

Master's Programme in Materials Science and Engineering

June 2023

The aircraft industry uses a high amount of composite materials and employs adhesive bonds extensively to join the different structures. Bonded joints do not require any mechanical drilling and are able to distribute the loads better than mechanical joints. The main challenge of adhesive bonds is that it is not possible to check their structural integrity once they are formed. Additionally, adhesive joints are very dependent on the surface treatments applied to the adherend before bonding. This is a problem, especially in such a safety-oriented industry like the aircraft one. Some methods have been developed to assure that the surface quality has the right characteristics for bonding, such as measuring the contact angle that a drop of water forms once it is deposited on the bonding surface.

This master's thesis aimed to investigate the correlation between the bond surface contact angle and the strength of adhesive bonds in carbon/epoxy composite laminates. This correlation could be useful in the aircraft industry for preventing weak adhesive bond joints by simply measuring the contact angle (CA) of the bond surface after the surface treatment and before even producing the adhesive bond joint.

To study the correlation, different surface treatments were applied to carbon/epoxy laminates and their CA was measured using a top-view and hand-held device. Single lap shear (SLS) and double strap joints (DSJ) were manufactured using epoxy adhesive and carbon/epoxy laminates. Finally, both types of adhesive joints were mechanically tested, recording their maximum load. After testing, their failure surfaces were studied. Additionally, the effect of exposing adhesive joints with different surface treatments to an elevated temperature wet (ETW) environment was also evaluated. The applied surface treatments varied in the surface roughness level, in the cleaning process and in the substances used to contaminate the bond surface. This variety in surface treatments achieved very different CA values.

Based on these results, CA measuring was able to distinguish clearly different surface roughness as well as different contaminants on the surface of carbon/epoxy laminates. DSJ highest strength results were obtained applying a baseline sanding, whereas cleaning the surface with a solvent reduced the bond strength as much as contaminating it. SLS testing strength results indicated an opposite trend, which could be influenced by strong peel forces in SLS samples and delamination as main failure mode. A not-unequivocal correlation was observed for the minimum CA of each DSJ sample and its corresponding testing strength, with low CA surface treatments leading to the highest bond strength. Samples exposed to ETW environment had lower strength and followed a CA-strength correlation like DSJ.

Keywords: Composite, Adhesive bond, Contact angle, Strength, Surface treatment

The originality of this thesis has been checked using the Turnitin OriginalityCheck service.

PREFACE

I would like to acknowledge and thank my supervisors for their support and guidance during the thesis work, as well as my co-researcher Franziska Mews for her altruistic assistance. I would also like to thank Tampere University and the Technical University of Madrid for giving me the opportunity to study this double master program in Materials Engineering, which I will be finishing with this master's thesis. Finally, I would also like to thank my parents for believing in me all these years and for always supporting me to keep studying, no matter if in Toledo, Madrid or Tampere.

Tampere, 22 June 2023

Daniel Blanco Garde

CONTENTS

1.INTRODUCTION	1
2.THESIS OBJECTIVES.....	3
3.COMPOSITES	4
3.1 Definition.....	4
3.2 Thermoset matrix.....	4
3.3 Reinforcing carbon fibres	5
3.4 Laminate.....	6
3.5 Joining composite materials.....	7
4.ADHESIVE BONDING	10
4.1 Principles of adhesive bonding.....	10
4.2 Surface preparation.....	10
4.3 Surface contact angle and energy for quality assessment.....	11
4.4 Environmental effect	14
4.5 Types of adhesive joints.....	15
4.6 Failure modes in adhesive joints	16
5.MATERIALS AND METHODS	19
5.1 Test matrix	19
5.2 Materials	20
5.3 Testing samples. SLS and DSJ adhesive joints	22
5.4 Surface treatments.....	24
5.5 Contact angle measurement procedure	29
5.6 Manufacturing	31
5.7 Environmental exposition after bonding.....	34
5.8 Mechanical testing	35
6.RESULTS & ANALYSIS.....	37
6.1 Contact angle results	37
6.2 Mechanical testing results	40
6.3 Failure surfaces analysis.....	43
6.4 Contact angle – bonding strength correlation	50
6.5 Environmental exposition results.....	54
7.DISCUSSIONS	59
8.CONCLUSIONS.....	63
REFERENCES.....	65

LIST OF FIGURES

<i>Figure 1: Evolution of carbon fibre composites use in commercial and military aircraft [1].....</i>	<i>1</i>
<i>Figure 2: Load capacity increases when adhesive and mechanical joints are used together [6].....</i>	<i>8</i>
<i>Figure 3: Example of contact angle measurement by placement of a water drop on the surface of a CFRP laminate (Courtesy of co-researcher Franziska Mews).....</i>	<i>13</i>
<i>Figure 4: Loading modes in adhesive joints [36].....</i>	<i>15</i>
<i>Figure 5: Different types of adhesive joints [6].....</i>	<i>16</i>
<i>Figure 6: Strength of different adhesive joints [6].....</i>	<i>16</i>
<i>Figure 7: Failure modes in ASTM D5573 standard for adhesive joints [42].....</i>	<i>17</i>
<i>Figure 8: From left to right, type-B and type-A laminates.....</i>	<i>20</i>
<i>Figure 9: P180 sanding paper used for surface roughening.....</i>	<i>21</i>
<i>Figure 10: From left to right, manufacturing tools for SLS and DSJ.....</i>	<i>22</i>
<i>Figure 11: Geometry and components of SLS samples.....</i>	<i>23</i>
<i>Figure 12: SLS sample with end-tabs already attached.....</i>	<i>23</i>
<i>Figure 13: Geometry and components of DSJ samples.....</i>	<i>24</i>
<i>Figure 14: Baseline level treatment process steps.....</i>	<i>25</i>
<i>Figure 15: Contamination process steps.....</i>	<i>28</i>
<i>Figure 16: SLS contaminated surfaces (A&B).....</i>	<i>28</i>
<i>Figure 17: DSJ contaminated surfaces (F&G).....</i>	<i>29</i>
<i>Figure 18: Surface Analyst contact angle measuring device.....</i>	<i>29</i>
<i>Figure 19: Water drops left on the surface of the laminate after CA measuring.....</i>	<i>30</i>
<i>Figure 20: Placing of FM 300-2 sheet on a type-A laminate while manufacturing a SLS sample.....</i>	<i>31</i>
<i>Figure 21: Vacuum bag inside the oven with thermocouples and vacuum ready for curing process.....</i>	<i>32</i>
<i>Figure 22: Temperature-time diagram of the FM 300-2 curing cycle obtained using 2 thermocouples.....</i>	<i>33</i>
<i>Figure 23: Schematic with measurement points of SLS (top) and DSJ (bottom) samples.....</i>	<i>33</i>
<i>Figure 24: SLS Grease ETW samples inside the environmental chamber.....</i>	<i>34</i>
<i>Figure 25: Thermal imager and thermal image obtained during ETW testing.....</i>	<i>35</i>
<i>Figure 26: DSJ sample clamped to the load cell just before testing.....</i>	<i>36</i>
<i>Figure 27: Average, maximum and minimum CA per surface treatment in SLS samples. SD is plotted as error bar in the average CA.....</i>	<i>37</i>
<i>Figure 28: Average, maximum and minimum CA per surface treatment in DSJ samples. SD is plotted as error bar in the average CA.....</i>	<i>38</i>
<i>Figure 29: Comparison of average CA and SD between SLS and DSJ samples.....</i>	<i>39</i>
<i>Figure 30: Comparison of the maximum average stress and SD between SLS and DSJ samples.....</i>	<i>41</i>
<i>Figure 31: Normalized strength comparison of DSJ and SLS surface treatments using the strength ratio.....</i>	<i>42</i>
<i>Figure 32: Representative surfaces of main failure modes.....</i>	<i>44</i>
<i>Figure 33: Representative failure surfaces of each surface treatment applied to SLS samples.....</i>	<i>45</i>
<i>Figure 34: Average failure mode in SLS samples.....</i>	<i>46</i>
<i>Figure 35: Representative failure surfaces of each surface treatment applied to DSJ samples.....</i>	<i>48</i>
<i>Figure 36: Average failure mode in contaminated DSJ interfaces.....</i>	<i>48</i>
<i>Figure 37: Side-by-side comparison of average failure mode in contaminated (C) and non-contaminated (NC) DSJ interfaces.....</i>	<i>49</i>

<i>Figure 38: Joint strength - Average CA comparison of DSJ samples</i>	50
<i>Figure 39: Joint strength - Maximum CA comparison of DSJ samples</i>	51
<i>Figure 40: Joint strength – Minimum CA comparison of DSJ samples</i>	51
<i>Figure 41: Joint strength – Average CA comparison of SLS samples</i>	52
<i>Figure 42: Joint strength – Maximum CA comparison of SLS samples</i>	53
<i>Figure 43: Joint strength – Minimum CA comparison of SLS samples</i>	53
<i>Figure 44: Comparison of the maximum average stress and SD between samples exposed to RTD and ETW environment</i>	54
<i>Figure 45: Comparison of RTA and ETW representative failure surfaces</i>	55
<i>Figure 46: Average main failure mode in ETW samples compared with RTA counterparts</i>	56
<i>Figure 47: Joint strength – Average CA comparison of SLS ETW and RTA samples</i>	57
<i>Figure 48: Joint strength – Maximum CA comparison of SLS ETW and RTA samples</i>	57
<i>Figure 49: Joint strength – Minimum CA comparison of SLS ETW and RTA samples</i>	58

LIST OF TABLES

<i>Table 1: Main characteristics of mechanical fastening and adhesive bonding of composites with thermoset matrix [6]</i>	<i>8</i>
<i>Table 2: Full test matrix with number of samples tested for each surface treatment and type of adhesive joint.....</i>	<i>19</i>
<i>Table 3: Laminate dimensions and characteristics.....</i>	<i>20</i>
<i>Table 4: Dimensions of SLS samples</i>	<i>22</i>
<i>Table 5: Dimensions of DSJ samples</i>	<i>24</i>
<i>Table 6: Average maximum stress and standard deviation per surface treatment and sample type.....</i>	<i>40</i>

LIST OF SYMBOLS AND ABBREVIATIONS

Avg.	Average
CA	Contact angle
CFRP	Carbon fibre reinforced plastic
DSJ	Double strap joint
ETW	Elevated temperature wet
HM	High modulus
HTS	High tensile strength
IM	Intermediate modulus
Light	Light sanding
Max.	Maximum
MEK	Methyl ethyl ketone
Min.	Minimum
NDI	Non-destructive inspection
Openlab	Open laboratory contamination
PAN	Polyacrylonitrile
PEEK	Polyether ether ketone
PMC	Polymeric matrix composites
PPS	Polyphenylene sulphide
R^2	Coefficient of determination
RTA	Room temperature ambient
SA	Surface analyst
SD	Standard deviation
SLS	Single lap shear
UHM	Ultra-high modulus
<i>i</i>	Number of testing sample

1. INTRODUCTION

The aircraft industry is well-known for using lightweight materials to keep the weight of the aircraft structure as low as possible, maximizing the fuel economy and the payload capacity as a direct consequence of such weight reduction. Lightweight materials are the ones that exhibit high mechanical properties, such as stiffness and strength, while having a low mass in a component or a structure. Common lightweight materials in aerospace applications are aluminium alloys and composites. Moreover, composite materials present higher lightweight characteristic than traditional aluminium alloys. This explains why the research and use of composites in the industry have been growing almost exponentially during the last 40 years. The growing trend in the use of composite materials in the aircraft industry is presented in Figure 1.

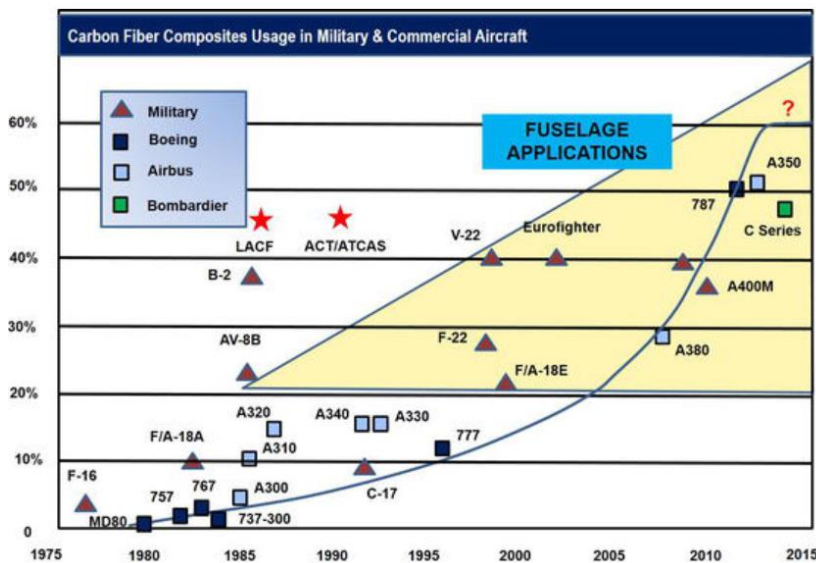


Figure 1: Evolution of carbon fibre composites use in commercial and military aircraft [1]

Composite materials are expected to increase their importance in the aircraft industry. Consequently, there is a lot of research for obtaining higher specific properties and higher recyclability to reduce the environmental impact of the aircraft industry and composite materials. These aspects will be especially relevant for the next generation of commercial aircraft currently on the design phase [1]–[4].

Composite structures are usually joined by using adhesive bonds, because they do not require any drilling and they are better at distributing the loads than mechanical joints.

Nevertheless, adhesive bonds are not free of challenges. Their main challenge is the inability to check their quality once formed: there is no inspection technique capable of determining whether a bond meets the quality standards or not once it has been produced. Additionally, adhesive joints are very dependent on the surface treatments applied to the adherend before bonding, and variations on the process could alter the pre-bond surface quality, resulting in a significantly lower joint strength. This is a problem, especially in such a safety-oriented industry like the aircraft one. Because of that, surface quality assessment techniques are being researched, whose task is to guarantee that the pre-bonding surface treatment has been the right one and that the surface is ready for bonding. One example of these techniques is surface contact angle measurement, which consists of placing a drop of water on the treated surface and measuring the angle that the drop forms with the surface. The measured contact angle (CA) can be used to assess if the surface is ready for bonding or not.

2. THESIS OBJECTIVES

The main research questions this thesis is trying to answer are the following:

- How does the strength of adhesive joints correlate with the surface quality of carbon-reinforced epoxy laminates?
- Is measuring the contact angle able to identify clean surfaces from contaminated ones? Moreover, is it able to identify if a cleaning solvent has been used in the surface?
- How does exposing adhesive joints to a hot and wet environment affect their bond strength?

To answer these questions, 2 types of adhesive joints with 8 different surface treatments will be manufactured and tested. Their joint strength will be determined by mechanical testing, whereas their surface quality will be determined quantitatively by measuring the contact angle of waterdrops on the composite surface. Moreover, 4 surface treatments will be used to contaminate the bond surface and assess if that contamination can be detected. Finally, the influence of exposing adhesive joints with different surface treatments to a hot and wet environment will also be studied and compared with the results obtained with adhesive joints at ambient environment.

Stablishing a solid quantitative correlation between adhesive joint strength and surface contact angle could increase the reliability of adhesive joints and solve one of the main problems of adhesive bonding.

3. COMPOSITES

3.1 Definition

Composite materials are combinations of different materials that have different composition and/or form, where each individual component retains its identity, without dissolving or merging into the other components [5].

In most composites there is a component that acts as the matrix of the whole composite. Composites can be classified depending on the nature of their matrix, which can be polymeric, ceramic or metallic. Nevertheless, polymeric matrix composites (PMC) are the most interesting ones due to their lightweight characteristics. The complementary element to the matrix is a reinforcing component, which can be classified depending on its shape: round, ellipsoidal, short fibres and long fibres.

The highest-performance composites used in the aerospace industry are PMC, with a combination of a thermoset resin matrix and a reinforcement based on high modulus continuous long carbon fibres [5]–[7]. The combination of a thermoset matrix and long-continuous carbon fibres allows this type of composites to achieve extremely high values of specific strength and specific stiffness. These two properties are key in all industries where lightweight materials are a must, such as in the space and in the aircraft industries [6], [7].

It should be noted that the properties of composite materials are quite different from traditional materials used in aircraft structures such as aluminium alloys. For example, metallic materials are usually completely isotropic, unlike composite materials, which are usually anisotropic: they have a higher strength and stiffness in one particular direction (fibre direction) but lower mechanical properties in perpendicular directions. This anisotropy can be balanced by stacking several layers as described in Chapter 3.4.

3.2 Thermoset matrix

The main task of the matrix is to hold the reinforcing fibres together, providing enough structural integrity to the composite material in a way that protects the fibres from external damage, distributing and transferring the loads applied to the composite between the different elements. In order to have good mechanical properties, it is important to ensure a solid interface-bond between the matrix and the fibre, either mechanically or chemically. Moreover, the matrix material should be chemically compatible with the fibres material to avoid chemical degradation and corrosion in the interface [8].

The main polymers used in aerospace composites are thermoset polymers, such as epoxies and polyesters. Thermosets production starts with a liquid solution of prepolymers and reactive monomers that solidifies irreversibly in the curing process, resulting in a 3D solid and a crosslinked structure that prevents the material from melting and flowing again, even if heat is applied to it. This crosslinked structure is not found in thermoplastics, whose structure is based on not-crosslinked polymer chains. As a result, thermoplastics soften and melt when the temperature is high enough, but harden later during the cooling down process [8].

Epoxy resins have good mechanical properties as well as good environmental resistance. One of their major disadvantages is that they are flammable unless additives are used to improve their burning characteristics. Nevertheless, they have a high thermal stability up to 200 °C and can be used in different composite manufacturing processes such as wet resin, prepreg and film adhesive layers [5]. Additionally, the toughness of epoxy resins can be further increased with some techniques like using small amounts of elastomers with a high molecular weight or adding micro and nano particles to it [9].

Nevertheless, there are some thermoplastics such as polyether ether ketone (PEEK) and polyphenylene sulphide (PPS) which have been intensively researched due to their interesting properties like their lower moisture absorption and their outstanding toughness. Their manufacturing is also simpler than the one for thermosets as well as their service temperatures: service temperature of epoxy resins is usually not much higher than 200 °C for aerospace applications whereas the melting temperature of PPS and PEEK is 278 °C and 360 °C, respectively [5], [8]. Additionally, since they are thermoplastics they could benefit from joining techniques not available for epoxy composites, such as thermoplastic welding and ultrasonic welding [10].

PEEK has a high thermal stability, an excellent resistance to solvents, chemicals and hot water. It can be used up to 250 °C for prolonged times in contact with the air, unlike other thermoplastic materials. It has a failure strain of 15% under tensile load and it has a high impact strength. Another advantage of PEEK matrix is that it can be manufactured with different techniques such as injection moulding, compression moulding and extrusion [11].

3.3 Reinforcing carbon fibres

Fibres are used in composite materials because they have a high stiffness, strength and low weight. Even if the matrix has an important role, the reinforcement fibres are respon-

sible of the main composite structural properties, such as the tensile, compressive, flexural strength and the stiffness. They are also the main load-carrying element of the composite. Reinforcing carbon fibres are solid and have a circular cross section. Usually, the smaller the carbon fibre diameter, the higher strength values can be achieved due to the smaller number of defects on the fibres [6], [7].

There are several types of materials available to be used as reinforcement fibres, but they can be divided into 3 groups: organic, ceramic and metallic fibres. Organic fibres are the ones with the best high strength and lightweight properties combination, making them the most interesting ones for the aerospace industry. Glass, aramid (Kevlar) and carbon fibres are considered organic fibres.

Carbon (or graphite) fibres are the most used fibres in aerospace composites due to their lightweight characteristics and excellent chemical resistance. Their mechanical properties depend on factors like the raw material and the manufacturing process. The main raw materials (or precursors) are polyacrylonitrile (PAN) and pitch. Although PAN fibres are more expensive than pitch fibres, they have 3-times higher strength, making them the most common fibres in the aerospace industry [12]. Carbon fibres are usually available in 3 main forms: high tensile strength (HTS), high modulus (HM) and ultra-high modulus (UHM). The type of fibre is chosen depending on the mechanical requirements of the structure to design as well as on the cost [6].

Carbon fibre reinforced plastics (CFRP) composites have better fatigue properties than aerospace-graded aluminium alloys as well as higher vibration damping characteristics. Additionally, using composites with carbon fibres allows the design of structures with null thermal expansion-contraction, eliminating possible thermal stresses [5], [6], [12].

3.4 Laminate

A lamina is formed by arranging unidirectional or woven fibres in a matrix to form a thin layer of composite material. This thin layer can be referred as lamina, ply or layer. A lamina with straight and parallel fibres is denominated as unidirectional ply. A unidirectional ply has its highest mechanical properties along the fibre direction, whereas it has its lowest mechanical properties in the direction perpendicular to the fibre direction. The reason for this anisotropy in mechanical properties is due to the different components working in each direction: fibres work mostly in the fibre direction, whereas the matrix is responsible for carrying the loads that are applied perpendicularly to the fibre direction. The orientation of a ply is determined by the angle between the ply fibres and the longitudinal direction of the ply, which can be any value between -90° and $+90^\circ$. By bonding

several plies together, a laminate is formed. The stacking sequence of the laminate is the order in which the different plies are bonded. The mechanical properties of a laminate are determined by its layers' orientation as well as its stacking sequence [7].

If the properties of the laminate want to be maximized in the main direction, then a uni-directional laminate composed exclusively of 0° plies is the best option. Nevertheless, many applications require balancing the load-carrying capability of the laminate in different directions using, for example, a combination of 0° , $+45^\circ$, 90° and -45° ply orientations. To obtain a completely balanced and quasi-isotropic laminate it is necessary to use the same number of plies in 0° , $+45^\circ$, 90° and -45° directions. This results in a laminate with the same mechanical properties in the fibre plane [13].

3.5 Joining composite materials

The aircraft composite structure is usually manufactured in several smaller parts to make the manufacturing process simpler. This design philosophy also has the advantage that if one part of the structure is damaged, it can be repaired ex-situ or substituted by another part without compromising the rest of the structure. This modular philosophy is quite cost-effective since it reduces costs during manufacturing and during the service life of the airplane. Nevertheless, it has a main disadvantage: the different parts of the structure must be bonded to each other tightly and securely enough to ensure that they are able to transfer the structural loads. The most common joining elements used in aircraft structures are fasteners, which is a type of mechanical joints [6].

Joints act as load transfer bridges between different aircraft structures. Because of that, they are responsible of distributing the loads between the different components and they are also responsible of the global structural integrity. In fact, this responsibility in load transfer is even more relevant when factors like stress concentration or secondary stresses due to eccentricities are considered. For these reasons, joints are one of the most common failure sources in aircraft structures and must be designed taking that into account.

Stress concentrations in joints are related to the loading around the holes due to the discontinuity in the structure, as well as the decreased area in the material in mechanical joints. On the other hand, stress concentrations in adhesive joints appear because of maintaining the strain compatibility between the different surfaces.

Another problem of joints is their weight. For example, even though the weight of a fastener is completely negligible when compared with the aircraft structure, the mass contribution of all the fasteners to the aircraft structure is considerable. Mainly for this reason,

adhesive bonding for composite materials with thermoset matrix have been developed, since they can provide a strength and weight advantage over mechanical joints like fasteners, although their weight in the final aircraft is not negligible either. A brief comparison between mechanical fastening and adhesive bonding for composites is presented in Table 1.

Table 1: Main characteristics of mechanical fastening and adhesive bonding of composites with thermoset matrix [6]

Method	Advantages	Disadvantages
Mechanical fastening	<ul style="list-style-type: none"> • Mature technology • Supplement to weld/bond assembly methods • Easy inspection 	<ul style="list-style-type: none"> • High weight • Requires sealing
Adhesive bonding	<ul style="list-style-type: none"> • Lower weight • Better stress distribution 	<ul style="list-style-type: none"> • Irreversible • Difficult inspection

Mechanical fastening and adhesive bonding are not completely substitutional, since both types of bonding can work together. For example, using fasteners and adhesive bonding in the same area significantly increases the loading capacity of the joint, as can be seen in Figure 2. This advantage can also be used to reduce the number of fasteners needed for a joint while keeping its loading capacity constant due to the additional adhesive bonding, resulting in a weight reduction [6].

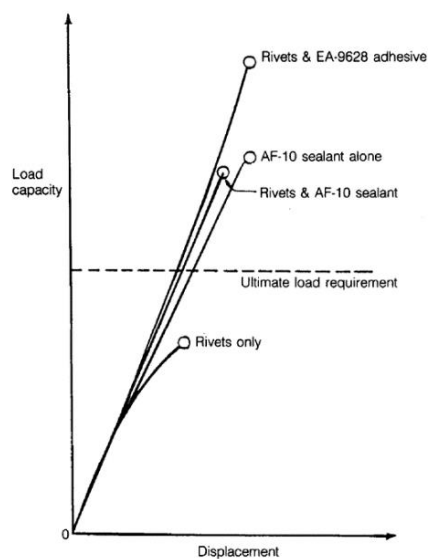


Figure 2: Load capacity increases when adhesive and mechanical joints are used together [6]

The most common type of mechanical joints used in aircraft structures is fasteners. Nevertheless, there are many types of mechanical joints and many materials available for mechanical joints. For using fasteners there are some rules regarding their positioning in the material. There has to be a minimum spacing between fasteners as well as a minimum distance between the fasteners and the edge of the material.

Another aspect that should be considered for fasteners is galvanic corrosion. This type of corrosion appears when incompatible materials are used. In the case of typical aerospace composites with carbon fibres as reinforcement, there is a high risk of galvanic corrosion of the fastener if the latter is made of, for example, steel and aluminium. For this reason, the most traditional material used for fasteners in carbon fibre composites is titanium. If the joint is not required to transfer high loads, composite fasteners can be used, with a significant decrease in weight. Additionally, the fasteners should be distributed in not more than two rows, because the low ductility of composite materials results in an uneven load transfer, with the outer rows of fasteners bearing the highest load transfer [6]. Moreover, fasteners increase the risk of delamination in CFRP laminates [14].

Adhesive joints are extensively used for joining composite parts to each other. They bond the different composite parts by transferring shear load between them. An advantage of adhesive bonding when compared with mechanical joints like fasteners is that they distribute the stresses more uniformly, preventing stress concentrations that could compromise the system's structural integrity [15]. Adhesive joints also act as sealants, have excellent corrosion resistance, do not require drilling and are lighter than mechanical joints. Nevertheless, they are irreversible, and their structural integrity cannot be checked, which limits their application in safety-orientated industries such as the aircraft industry. Adhesive joints and adhesive bonding are studied in more detail in Chapter 4.

4. ADHESIVE BONDING

4.1 Principles of adhesive bonding

Before discussing the principles of adhesive bonding, it is important to provide a definition for adhesion. Although it is still a source of debate, one of the best definitions for adhesion is the one proposed by Wu [16]: “Adhesion refers to the state in which two dissimilar bodies are held together by intimate interfacial contact such that mechanical force or work can be transferred across the interface. The interfacial forces holding the two phases together may arise from van der Waals forces, chemical bonding, or electrostatic attraction. The mechanical strength of the system is determined not only by the interfacial forces, but also by the mechanical properties of the interfacial zone and the two bulk phases.”

This adhesion state is reached by applying a material to the surfaces that are going to be bonded. The bonding material is known as adhesive, and the substrates that are bonded are denominated adherends [17]. The task of the adhesive is to join the substrates together and to transmit the stresses from one to another.

The basic and main requirements to obtain a good adhesive bond are the following [18]:

- A proper choice of adhesive.
- A good joint design.
- A proper cleaning of the substrate surfaces.
- A proper wetting of the surfaces to be bonded by the adhesive.
- A proper adhesive bonding process, including its solidification and curing processes.

4.2 Surface preparation

To improve adhesive bonding, a surface treatment is performed before the actual bonding. This surface treatment can be composed of one or several processes such as cleaning, removal of loose material, physical or chemical modification of the surface. It is especially important in CFRP bonding to remove the contamination that might be present on their surface like dust, dirt, fingerprints, lubricants and release agents [5], [6].

In the case of bonding CFRP composites, the surface treatment objective is to improve the bond by increasing the surface polarity, the surface wettability and by creating sites

for the adhesive on the surface [15]. The main reasons to apply surface treatments before bonding are the following:

1. To remove loose particles such as contaminants from the surface to be bonded.
2. To increase the molecular interaction between the adhesive and the adherend, as well as to optimize the adhesion forces from the adhesive-adherend interfaces.
3. To create a specific microstructure on the substrate more suitable for adhesive bonding.

A common surface treatment for CFRP composites is mechanical abrasion. The principle behind this surface treatment is that abrading the surface produces a clean surface while also increasing the contact area between the adhesive and the substrate. It can be carried out by sanding or by grit blasting, and its main advantages are its simplicity and that it can be performed for field repair works [6]. After the abrasion process, it is important to remove the loose particles on the substrate surface before bonding. This can be done, for example, by wiping in one direction with a dry cloth or with a cloth moistened with a solvent, such as methyl ethyl ketone (MEK) [15]. A more novel cleaning technique is the one applied in Wang et al. [19], which consists in a ultraviolet-ozone cleaning treatment right after sanding the laminates, improving significantly the bonding strength of CFRP laminates as a result. This ultraviolet-ozone treatment was highly effective in removing the organic contaminations still present on the surface after sanding without modifying the roughness of the laminate.

Peel ply removal is also a very typical surface treatment for composite laminates, where one or both outer layers of the laminate are specifically designed to be removed or peeled easily. The purpose of this peel ply is that it can be removed when the laminate is going to be bonded, preventing any contaminants to adhere to the bonding surface. This technique is usually preferred to mechanical abrasion because there is a lower risk of contamination presence on the surface and a lower risk of damaging the fibres. The material used to manufacture the peel ply has to be compatible with the matrix material and has to be easy to remove without damaging the fibres of the composite [5], [6].

4.3 Surface contact angle and energy for quality assessment

Adhesive joints are difficult to inspect once they have been manufactured: visual inspection cannot be carried out and other more complex non-destructive inspection (NDI) techniques are unable to detect weak bonds, which are the bonds that fail in the adhesive-adherend interface. For that reason, adhesive bonding is recognized in the ISO 9001

[20] quality standard as a “special process”, because it is a process “in which the result cannot be fully verified by subsequent monitoring and measurement or non-destructive testing of the product”. Because of this, it is necessary to perform a complete planning of the process where all the error-inducing factors are included to prevent errors from happening. ISO 9001 is a general quality standard that does not apply only to adhesive bonding, but also to other processes such as welding. DIN 2034-1 [21] is a standard which specifies the requirements for assuring the quality of load-carrying adhesive bonds along all the bonding process, from development to manufacturing and also later repair works. Additionally, companies from the aerospace industry have developed their own quality standards for adhesive joints. These standards are empirical, based on the manufacturing of adhesive joints and the strength results obtained from their mechanical testing. If the bond strength measured is above the acceptance limit established by the company, then it is considered a good bond. The main problem of this type of tests is that they are inherently destructive.

There are some surface quality inspection techniques whose aim is to assure that the joint strength will be good enough before the bonding is even conducted. Complementarily, they also aim at preventing the formation of weak bonds. One of the most traditional and simplest techniques used for these purposes is water-break test, which is a **qualitative** test that relies on the premise that clean surfaces will hold a continuous film of water, whereas not-clean surfaces will hold discontinuous water droplets and produce a “break” in the water film. If the surface presents a continuous film of water, then it is ready for bonding. Interpreting results from water-break test is not always straightforward and becomes more difficult when assessing narrow surfaces due to the reduced area [22].

Contact angle measurement is another surface quality method, but unlike water-break test it has the advantage of being a **quantitative** method. Measuring the contact angle (CA) that a drop of liquid presents on a treated composite surface (as seen in Figure 3) provides useful information about its surface energy. For example, if the CA that the drop forms is very small it is indicating that the surface energy is quite high, meaning that it should perform better at bonding [15]. Nevertheless, the relationship between CA and surface energy is not always straightforward, as seen in Bechikh et al. [23], where they do not share exactly the same trends.

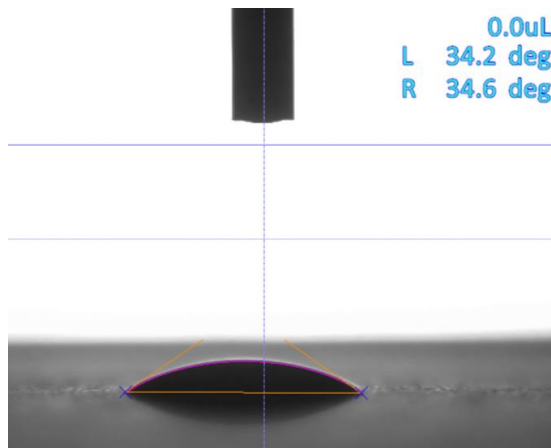


Figure 3: Example of contact angle measurement by placement of a water drop on the surface of a CFRP laminate (Courtesy of co-researcher Franziska Mews)

Measuring the surface CA can also provide information on whether the surface is contaminated or clean: contaminated surfaces tend to have higher CA values whereas clean surfaces usually present lower CA values than their contaminated counterparts, as some studies suggest [24] [25]. For these reasons, measuring the surface CA can be a valuable tool to assess if the surface treatment prior bonding has been correctly applied.

Moreover, since CA measurement provides quantitative values, it is numerically possible to develop a correlation between the surface CA and the bond strength, and there are several research papers about this topic. For example, Sun et al. [26] results show that laser-treated composite surfaces had a lower surface CA and a higher adhesive joint strength than the untreated composite surfaces. Nevertheless, not all the references had such a straightforward CA-strength relationship. Bechikh et al. [23] studied the strength single lap shear adhesive joints and their surface energy before bonding. The results were that the strength increased as the surface energy did. Nevertheless, the surface energy did not follow exactly the same trend as the CA. Unlike the previous reference, in Yang et al. [27] the surface CA followed the same trend as the surface energy. They tested both scarf joints and single lap shear joints. The highest strength of scarf joints was obtained for the minimum CA and maximum surface energy, whereas the highest strength of single lap shear joints was obtained with almost the lowest CA surface and almost the maximum surface energy. Finally, some references like Akman et al. [28] found out that a very low CA does not guarantee a high bond strength: their results show that using excessive laser power produced a surface with very low CA, but extremely poor joint strength.

Related with the previous comments about contamination-CA relationship, Dighton et al. [25] could identify contaminated surfaces from the clean ones due to their higher CA values. Moreover, the contaminated surfaces performed worse in adhesive joint strength

than their clean counterparts, thus obtaining a CA-strength correlation similar to previous Sun et al. [26]. Nevertheless, this CA-strength correlation was inconclusive when analysing only the different clean surfaces.

It should be noted that the CA can only be a useful indicator of the mechanical properties of a bond when the failure is in the adhesive-substrate interface. CA measurement loses its possible strength-indication relevance when the breaking of the bond is within the adhesive or within the substrate: it cannot provide information about the adhesive's internal strength nor about the substrate's delamination strength. Nevertheless, when these types of failure occur it means that the bonding was good. For example, in Pascal et al. [24] some adhesive bonds with low CA failed by delamination, obtaining lower strength values than the bonds with higher CA. which failed cohesively. Nevertheless, a CA-strength correlation was observed for the samples that failed in the adhesive-substrate interface: surfaces with higher CA values performed worse in peel strength tests than the surfaces with lower CA. On the other hand, Flinn et al. [29] could not find a clear correlation between the surface CA measurements and the adhesive bond quality.

4.4 Environmental effect

The initial bond strength of an adhesive is not guaranteed to remain the same during all its lifetime. Other than the before mentioned pre-bond surface treatments, the bonding strength of adhesive joints also depends on the environmental conditions that it experiences during its service life, which can degrade it [30]. The study of this environment-induced in aircraft components is challenging since their working environmental conditions are diverse and dynamic. For example, an aircraft could take-off from an airport in a hot-and-wet environment in a tropical area and finish its flight on a cold-and-dry environment. The same could be said for the radiation, which is significantly higher when the aircraft is at cruising altitude due to the thinner atmosphere above it. Additionally, operating in an airport close to the sea is linked with an increase of salinity in the environment which can enhance the corrosion of some aircraft components. Several studies have been done about this topic, especially in the case of CFRP adhesive joints, since CFRP is the material that can benefit the most from the implementation of adhesive joints in primary aircraft structures. Several research papers have studied the behaviour of such joints at different conditions like room temperature ambient (RTA), dry (RTD) and wet (RTW) environments; elevated temperature dry (ETD) and wet (ETW) environments, and also cold temperature dry (CTD) environment. For example, Knight et al. [31] exposed CFRP single lap shear adhesive joints to a ETW environment and that reduced their apparent shear strength in approximately 43% when compared with RTA samples. In Liu

et al. [32] double lap shear joints were exposed to 4 different environments, obtaining the highest strength with RTD followed by RTW, ETD and finally ETW. These results indicate that both elevated temperature and high humidity conditions degrade substantially the strength of adhesive joints. This problem with adhesive joints in ETW conditions is not restricted to composite samples, since Zhang et al. [33] also recorded a substantial decrease in the strength of single lap shear joints made of aluminium when exposed to a ETW environment. Nevertheless, other references obtained the opposite results. This is the case of Park et al. [34], which compared the strength of CFRP single lap shear joints with 4 different types of adhesives in 3 different environments: RTA, ETW and CTD. The obtained results were that 3 of the adhesives performed the best in the ETW environment and performed the worst in the CTD environment. The higher strength in ETW environment is attributed to the increased delamination strength of the tested laminates after ETW conditioning.

The bonding strength of adhesive joints done with CFRP materials is also dependent on factors such as the intensity of the loads during service, the density and the size of defects in the joint (such as de-bonds, delamination and pores), the physic-chemical properties of the adhesive bond and also the type of adhesive joint [35].

4.5 Types of adhesive joints

Adhesive joints can be loaded in different modes like shear, tension, cleavage and peel, which are presented in Figure 4. Nevertheless, adhesive joints are usually strongest in shear loading. For that reason, adhesive joints are usually optimized to load the adhesive mainly in shear and to minimize the other loading modes [36].

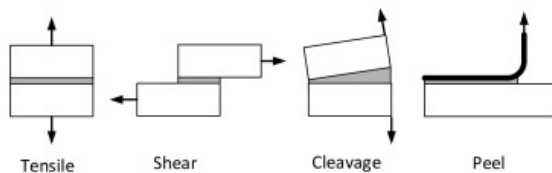


Figure 4: Loading modes in adhesive joints [36]

There are several different types of adhesive joints as seen in Figure 5, but the most common and simplest one is the single-lap joint (Figure 5.a). It is also denominated as single lap shear (SLS) because the load transfer between the substrates results mainly in a distribution of shear stresses. Nevertheless, there is also a powerful bending moment in the joint area due to the misalignment between the loading action lines. This bending moment generates peeling stresses normal to the adherend-adhesive interface, but it can be mitigated by adding end tabs to the SLS joints. Moreover, in the adhesive

layer there is also an axial stress distribution. The shear, peel and axial stress distributions reach their highest values close to the lap ends. Because of all these additional stress distributions, SLS joints are not the most suitable method to assess the shear strength of an adhesive [37].

More complex adhesive joints such as the double-strap joint (DSJ) (Figure 5.e) and the tapered strap joint (Figure 5.f) do not experience a bending moment and the resulting peel stresses are not as intense as the ones of SLS. This results in an increase of the joint strength that can be observed in the graph from Figure 6 and a failure mainly due to shear stresses. There are even more complex and stronger adhesive joints such as the stepped-lap joint (Figure 5.g) and the scarf joint (Figure 5.h), but their manufacturing is quite complex, reducing their applications. The two most common joints used for adhesive testing are SLS and DSJ, whose respective testing standards are ASTM D5868 [38] and ASTM D3528 [39].

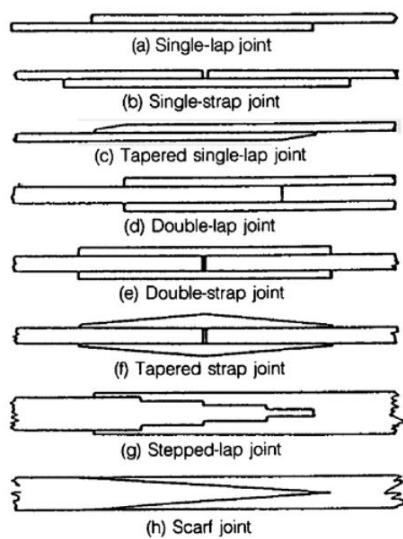


Figure 5: Different types of adhesive joints [6]

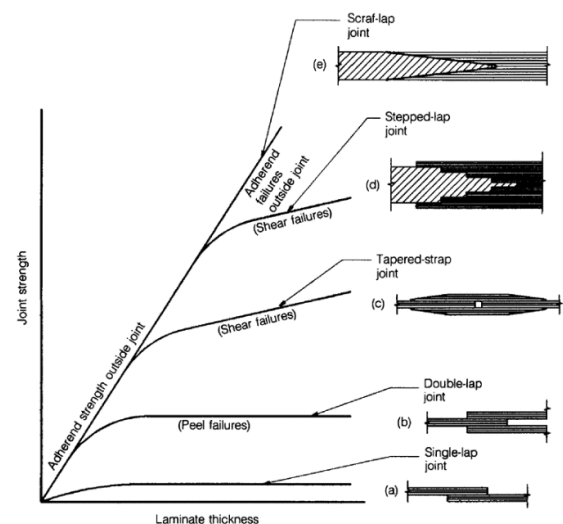


Figure 6: Strength of different adhesive joints [6]

Even though the strength of adhesive joints does not depend on the overlap size, it is necessary to have a minimum overlap size to prevent the adhesive in the middle of the joint from creeping [40], [41].

4.6 Failure modes in adhesive joints

Adhesive joint failure modes are categorized based on the ASTM D5573 [42] standard, which defines 7 different failure modes, of which 6 are presented in Figure 7.

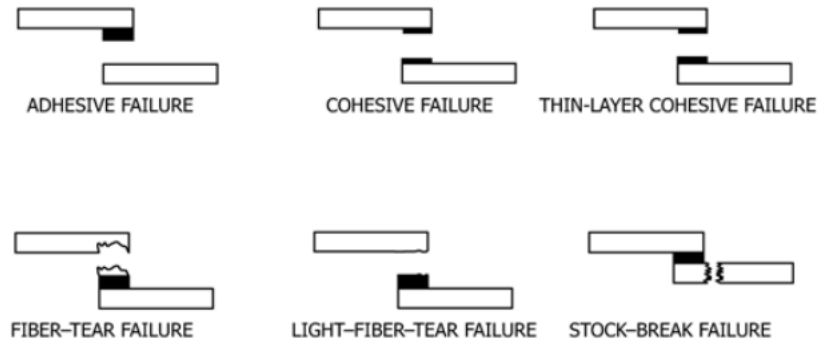


Figure 7: Failure modes in ASTM D5573 standard for adhesive joints [42]

This standard also provides the following descriptions of each type of failure, making their identification easier:

- Adhesive failure: failure at the interface between the adherend and the adhesive layer. Also known as interfacial failure.
- Cohesive failure: failure within the adhesive, leaving both adherends covered with an adhesive layer.
- Thin-layer cohesive failure: similar to cohesive failure, but the failure is very close to the adhesive-adherend interface. This results in a thin layer of adhesive on one of the adherends and a thick layer of adhesive on the other.
- Fibre-tear failure: failure occurs within the FRP substrate. Characterized by the presence of reinforcing fibres on both fracture surfaces.
- Light-fibre tear failure: failure occurs within the FRP matrix but near the surface. Characterized by the presence of a thin layer of FRP matrix visible on the adhesive with few or no substrate fibres on the adhesive.
- Stock-break failure: failure within the FRP substrate outside the adhesive joint region.
- Mixed failure: any combination of 2 or more of the previously identified failure modes.

When an adhesive joint fails, usually more than 1 failure mode is involved (mixed failure). Because of that, it is necessary to assess how much failure surface presents each type of failure mode. To quantify the importance of each failure mode, their contributions are provided as percentages of the total failure area. Nevertheless, it should be noted that weak bonds are characterized by failure in the interface between the adhesive and the adherend, i.e., by adhesive failure [43].

The failure mode is an important parameter to study if the failure of an adhesive joint is a consequence of an incorrect surface treatment or due to a weak boundary layer. It can also help interpreting and comparing stress results of adhesive joints better. Nevertheless, the failure mode is not as important as the maximum stress sustained by the adhesive joint, because some adhesive-adherend combinations might fail adhesively and still reach higher stress levels than other adhesive-adherend combinations with a weak adhesive that fails cohesively [43].

5. MATERIALS AND METHODS

The aim of this thesis is to assess the effect of different surface treatments on the bonding strength of adhesive joints while also looking for a correlation between the joint strength and the surface contact angle. In order to achieve these objectives, several surface treatments are applied to CFRP laminates, and the resulting surface contact angle is measured. Then, both SLS and DSJ are manufactured using treated CFRP laminates and are later mechanically tested, obtaining their bonding strength. It also aims at understanding how adhesive joints with the same surface treatment perform in mechanical testing after exposing them to different environments.

5.1 Test matrix

The whole test matrix of this thesis is presented in Table 2, where the number of tested samples per surface treatment and per type of adhesive joint is presented. In total, 90 samples divided in 8 different surface treatments are tested. Of those 90 samples, 51 are SLS adhesive joints and the remaining 39 are DSJ. Only 6 samples are exposed to elevated temperature wet (ETW) environment, whereas the remaining 84 are exposed and tested at room temperature ambient (RTA) conditions. Only 4 DSJ Light sanding samples were tested correctly due to not being able to properly test the remaining sample.

Table 2: Full test matrix with number of samples tested for each surface treatment and type of adhesive joint

Surface treatment	SLS	DSJ
Baseline	10	5
Light sanding	5	4
Openlab	5	5
MEK1	5	5
MEK4	5	5
Jet fuel	5	5

Hydraulic fluid	5	5
Grease	5	5
Baseline (ETW)	3	
Grease (ETW)	3	
Total per adhesive joint	51	39

5.2 Materials

All the laminates used in this project are made of carbon fibre reinforced plastic (CFRP) with a thermoset epoxy matrix and continuous carbon fibres as reinforcement. The CFRP material commercial designation is AS4/3501-6. All the laminates are manufactured by the same supplier (Patria). Additionally, all laminates include a peel ply attached to both sides/faces of the laminate. There are 2 different types of laminates used in this project, type A and type B, whose properties are presented in Table 3 and in Figure 8.

Table 3: Laminate dimensions and characteristics

Laminate type	Length (in 0° direction)	Width	Thickness	Stacking sequence
A	6"	6"	1.1"	[0/0/0/45/-45/0/0/45/-45/0] _s
B	3.1"	6"	0.55"	[0/0/0/45/-45] _s

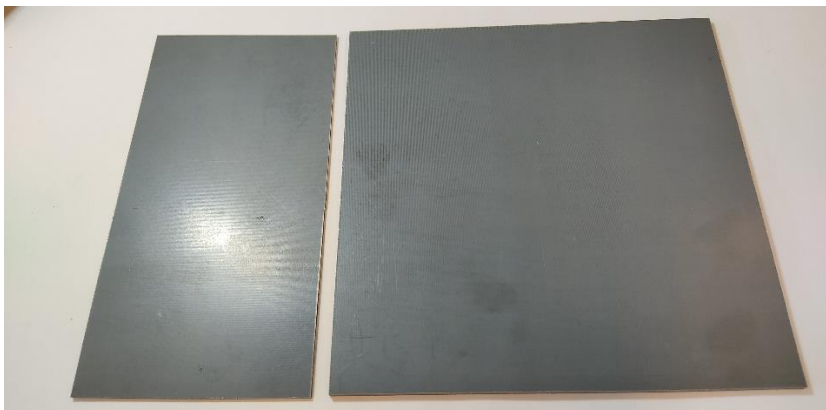


Figure 8: From left to right, type-B and type-A laminates

In order to create the different testing adhesive joints, it is necessary to bond them with an adhesive. The adhesive film used to bond the laminates is the FM 300-2, produced

by Solvay. This epoxy adhesive has a good toughness, and it can work in a wide temperature range, from -55 to 149 °C. Its official curing cycle is 1.5 hours at 121 °C, and the recommended maximum storing temperature is -18 °C [44]. Before using it, it is recommended to put it at room temperature for at least 2 hours to prevent it from absorbing an excessive amount of moisture.

The contaminants used for the difference contamination surface treatments are JP-8 MIL-DTL-83133 for jet fuel contamination, ROYCO 782 MIL-PRF-83282D for hydraulic fluid contamination and NYCO Grease GN 22 for grease contamination. Regarding MEK cleaning solvent, it was also provided by Patria.

Other than the main materials used for this thesis, it was necessary to use other materials for applying the surface treatments as well as for preparing and curing the adhesive joints. For example, P180 sanding paper (Figure 9) was used to manually roughen the surface of the CFRP laminates.

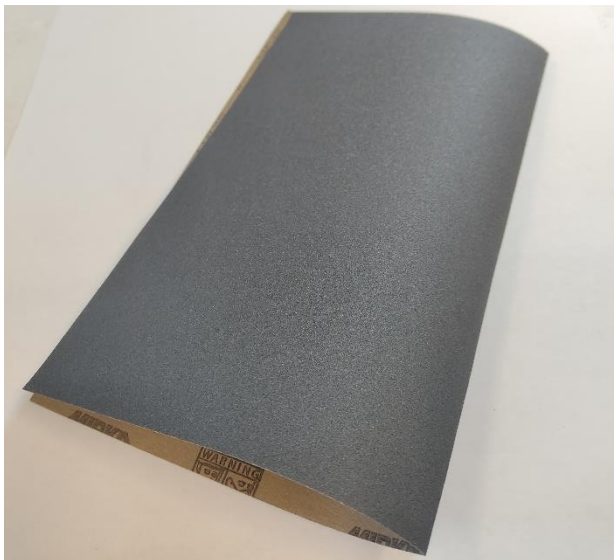


Figure 9: P180 sanding paper used for surface roughening

The thermocouples used to measure the adhesive joint temperature during curing are K-type and can withstand the curing temperatures without degradation or malfunctioning. The temperature readings done by the thermocouples were transmitted to a computer where they were recorded and saved.

There are 4 material types needed to manufacture the vacuum bag for curing:

1. The vacuum or bagging film WL7400, which is the outermost layer of the vacuum bag and the one responsible of assuring vacuum around the adhesive joint.

2. The release ease 234 TFP, whose main task is to provide an easy release barrier between the laminate and the breather film. It also protects the vacuum film from the sharp edges of the CFRP laminates that could damage it.
3. The breather film N10 purpose is to absorb the excess adhesive that might be released from the joint during curing.
4. The task of the sealing tape task GS 213 is to seal the vacuum bag. It must not degrade during the curing in the oven.

For manufacturing both SLS and DSJ, it was necessary to use some modified laminates that served as tools for the assembly of the adhesive joints. Not only that, but they also helped in the adhesive fillet formation due to their 45° edge. Additionally, they limited the bonding size and fixed the adhesive joint during the curing process. The modified laminates were not the same for both types of adhesive joints. Figure 10 shows the characteristic 45° edge for fillet formation of both manufacturing tools.

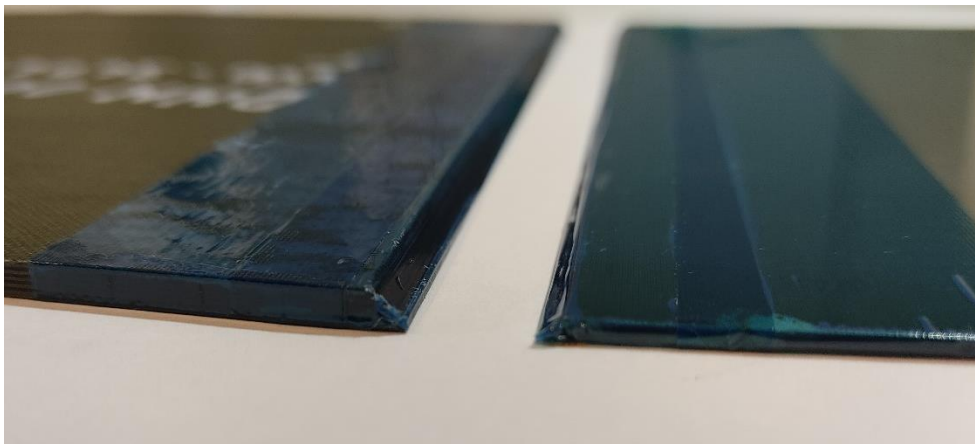


Figure 10: From left to right, manufacturing tools for SLS and DSJ

5.3 Testing samples. SLS and DSJ adhesive joints

As introduced previously, both SLS and DSJ were manufactured to serve as testing samples. The materials needed to produce SLS joints are not numerous: only two type-A laminates and a sheet of FM 300-2 adhesive are necessary. In Table 4 the dimensions of SLS samples as well as the amount of FM 300-2 adhesive used are presented. Figure 11 shows the geometry of a SLS sample, as well as its components, the orientation of the laminates and its bonding surfaces (A and B).

Table 4: Dimensions of SLS samples

Overlap length (")	0.5
--------------------	-----

Adhesive number of plies;	1;
Dimensions (“)	0.5” length x 1” width
Width (“)	1
Overall length (“)	11.5
Clamping length (at each end) (“)	1

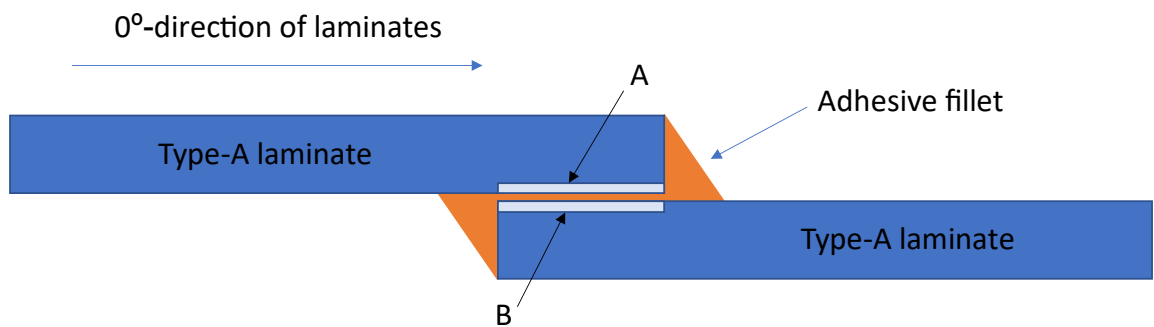


Figure 11: Geometry and components of SLS samples

To test the SLS samples in the available testing cell it is necessary to add tabs to their ends (end-tabbing). The result of this end-tabbing process can be observed in Figure 12. Unlike SLS samples, DSJ ones do not require end-tabbing for testing.

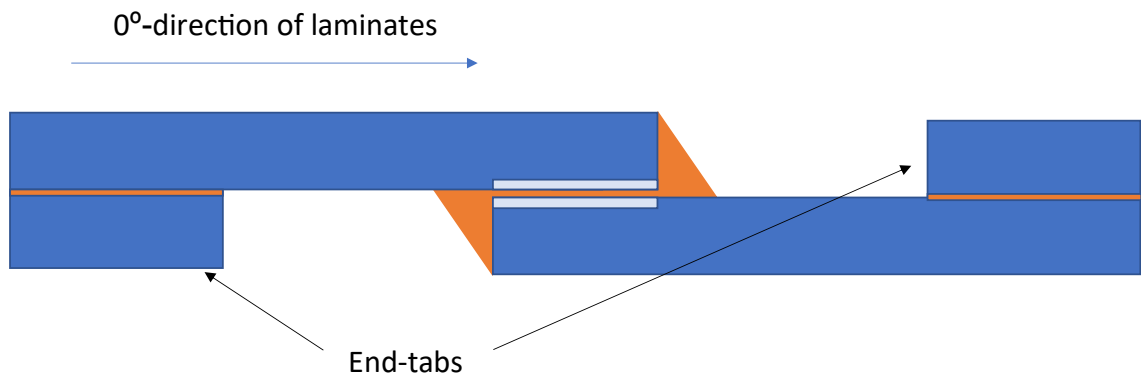


Figure 12: SLS sample with end-tabs already attached

The materials needed to produce DSJ samples are more numerous than in the case of SLS ones. They require two type-A laminates as parent laminates but also two stripes of type-B laminate as straps and a Teflon spacer to avoid the adhesive bonding between both parent laminates. They also need 2 sheets of FM 300-2 adhesive, one for each bonding line. The dimensions of DSJ samples are presented in Table 5. The geometry,

laminates orientation, components and bonding surfaces (A-H) of a DSJ sample can be observed in Figure 13.

Table 5: Dimensions of DSJ samples

Overlap length (“)	0.5
Adhesive number of plies per bonding line; Dimensions (“)	1; 1.118 length x 1 width
Teflon spacer length (“)	0.118
Width (“)	1
Overall length (“)	12.118
Clamping length (at each end) (“)	1

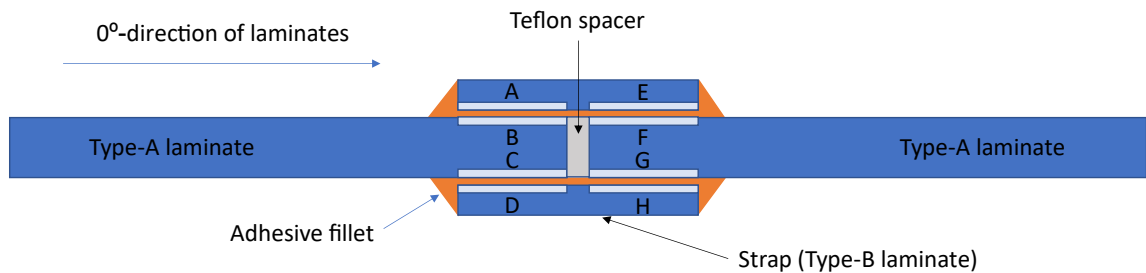


Figure 13: Geometry and components of DSJ samples

Although the width of both SLS and DSJ samples is 1”, they are manufactured as batches of 6”-width to simplify the manufacturing process. To avoid the worse bonding quality of the edges, only 5 1”-wide testing samples (and not 6) are obtained from each batch. This ensures that the bonding of the testing samples is more homogeneous, increasing the reliability of the later testing data.

5.4 Surface treatments

The CFRP laminates of this project received different surface treatments that could differ in aspects like the roughening level of the surface or the presence of some contaminant on the surface. Nevertheless, every surface treatment starts with the removal of the peel ply of both sides of the CFRP laminates.

Baseline level treatment

The baseline surface treatment (Baseline) is the one used as reference to compare the other surface treatments with. It consists of a roughening or sanding in random direction that is deep enough to eliminate the pattern left on the laminate by the already removed peel ply. In this roughening an important amount of black dust is produced due to the sanding of some carbon fibres. Figure 14.a is a visual example of the sanding process. Once the sanding is finished, the dust is removed from the surface by wiping it away with a dry cloth in just one direction, as seen in Figure 14.b. The bonding of the samples with a baseline surface treatment is done as soon as possible, to avoid any contamination from the environment.



a) Sanding of laminate to Baseline level b) Removal of sanding dust

Figure 14: Baseline level treatment process steps

Light sanding

The main difference of light sanding treatment (Light) with baseline treatment is that the sanding is shallower. As a result, the peel ply pattern on the substrate surface is not completely eliminated. The key to know when the sanding is deep enough for this surface treatment is the appearance of black dust from the carbon fibres: once that black dust appears, the sanding is completed. The dust generated during the roughening of the surface is eliminated from the surface with the same technique previously described for baseline sanding. As in the case of baseline, the sanding is done in random direction and the bonding of the samples with this surface treatment is done almost immediately to avoid any environmental contamination.

Open laboratory contamination

The open laboratory contamination (Openlab) surface treatment is almost the same as the baseline one, but they differed on the time between sanding and bonding: while in the case of the baseline surface treatment the bonding was done almost immediately

after the sanding had been finished, in the case of the open laboratory contamination the samples are left on the laboratory for 2 hours before bonding. This exposes the already-sanded surfaces to the contamination agents that are present in the environment of the laboratory. The idea behind this surface treatment is to try to assess the impact of a small time-break (e.g., a lunch break) between the surface sanding and the adhesive bonding of CFRP parts.

MEK cleaning

Methyl ethyl ketone (MEK) or butanone is an organic compound that is commonly used as an industrial solvent. Additionally, it is employed in the aerospace industry to clean the surface of composite parts before bonding them. For that reason, it is relevant to study the influence that MEK-cleaning has on the bonding strength.

Two types of MEK surface treatments were performed, denominated as MEK1 and MEK4. In both treatments the first step is to apply a baseline level surface treatment and then cleaning it with MEK. This MEK cleaning is done by wiping the laminate surface in one direction with a cloth previously moistened with MEK. After that step, the differences between the MEK1 and MEK4 processes appear. In MEK1, the MEK-cleaned surface is also wiped in only one direction but this time with a water-moistened cloth, with the purpose of eliminating the MEK from the laminate surface. After that, the laminate surface is flushed with water with the aim of removing all the MEK in the surface. Finally, a water break test is conducted to check that the surface is clean. Meanwhile, in MEK4 treatment no further action is performed after wiping the surface with MEK.

Other contaminations: Jet fuel, Hydraulic fluid and Grease

The last series of surface treatments are related to contaminants that can be found in an aeronautic working environment, like the hydraulic fluid used in the aircraft hydraulic system, the jet fuel stored inside the wings and the grease used for lubricating different aircraft systems. These contaminants are added after applying a baseline treatment to the laminate (see Figure 13 a), but the contamination process details depend on the state of the contaminant.

If the contaminant is a liquid, such as hydraulic fluid or jet fuel, then the contaminant is poured onto a cotton piece inside a beaker until soaking it (Figure 13 b). Once the cotton piece is soaked, it is removed from the beaker and held over it for 40 seconds (Figure 13 c). After that, the cotton piece is rotated to avoid a concentration gradient on it and held for another 20 seconds. Then, the cotton piece is placed for 60 seconds on the laminate surface that has already been sanded, as seen in Figure 13 d. Finally, a dry cloth is used to wipe in one direction over the contaminated area, like in Figure 13 e, until

no visual indication of the contaminant is present on the surface. The contamination treatment also wets the CFRP laminate as seen in Figure 13 f.



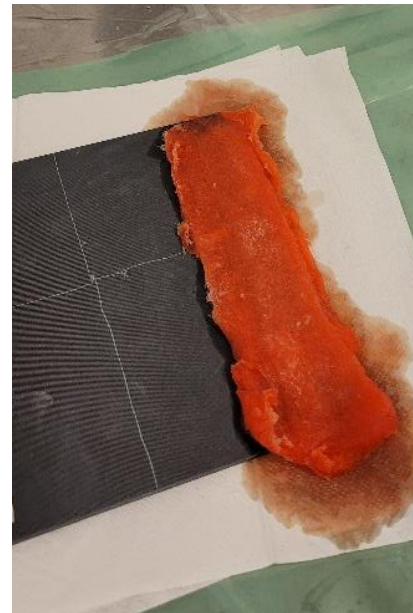
a) Laminates after baseline treatment



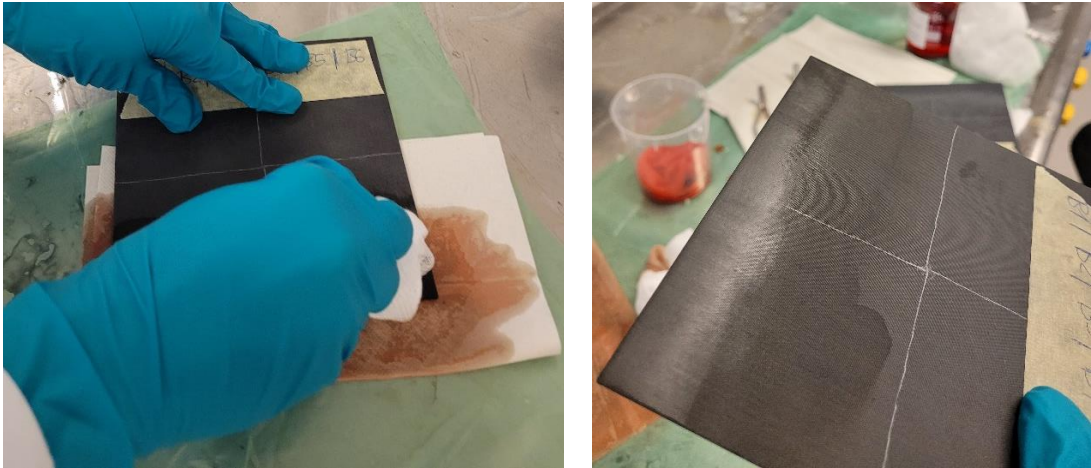
b) Pouring of hydraulic fluid inside a beaker with cotton



c) Removal of cotton from beaker



d) Placing of cotton on bonding surface



e) Wiping of contaminated surface with a dry cloth f) Final look of contaminated plate after wiping

Figure 15: Contamination process steps

On the other hand, for solid contaminants (grease) a wood spoon is used to put some grease onto a dry cloth. This dry cloth is used to distribute the contaminant by wiping the treated surface until all its area is covered with the contaminant. After that, the same cleaning process with a dry cloth previously described for liquid contaminants is performed.

Application of surface treatments in SLS and DSJ samples

In SLS samples, all the surfaces to be bonded receive the same surface treatment (A and B from Figure 16). Unlike the case of SLS samples, in DSJ samples not all the bonding surfaces receive the same surface treatment. Surfaces F and G receive the corresponding cleaning or contamination treatment, as seen in Figure 16, whereas the rest of the surfaces only receive a Baseline level surface treatment. This does not apply to Baseline, Light sanding and Openlab surface treatments, where **all** the surfaces from DSJ samples (A-H) receive the same surface treatment.

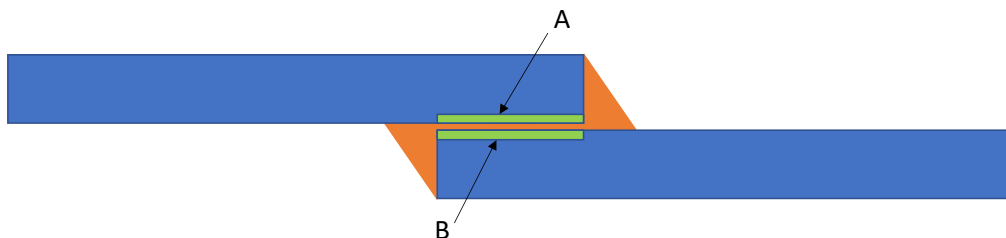


Figure 16: SLS contaminated surfaces (A&B)

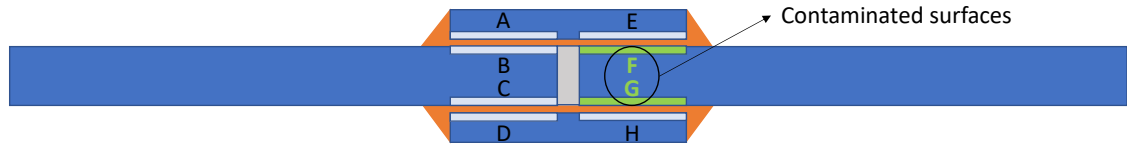


Figure 17: DSJ contaminated surfaces (F&G)

5.5 Contact angle measurement procedure

The contact angle (CA) of the treated surfaces is measured with a portable device denominated Surface Analyst (SA), developed by the company BTG labs and presented in Figure 18. The SA is a top-view device that measures the CA by taking a picture of the generated drop of water from above. In terms of operation, the SA software is easy to use, and the reduced size of its measuring head makes the device quite easy to handle. Additionally, SA is a portable and commercially available CA measuring device, which makes it quite interesting since this thesis is aimed to provide industry-applicable results.



Figure 18: Surface Analyst contact angle measuring device

The CA is measured after the corresponding surface treatment is applied to the laminate and after waiting a 15-minutes dwell time. Then, all the bonding surfaces of SLS and DSJ batches are measured. The purpose of this dwell-time is to standardize the CA measuring procedure, since the CA varies depending on the dwell time [25].

The CA measurements are taken every 1" of the measured laminate. In the case of laminates used for SLS batches, 2 CA measurements are taken in the bonding area per inch. Only 1 CA measurement in the bonding area is taken per inch in the laminates used for DSJ. Since all the laminates are 6" wide, it means that there are 6 CA measurement areas per laminate and per batch. Nevertheless, only 5 testing samples are obtained per batch. To solve this mismatch between number of CA measurement areas and testing samples, a relationship between them is established. This relationship is expressed in Equation (1), where i is the number of the testing sample, which ranges from 1 to 5.

$$\begin{aligned} \text{Testing sample CA data } (i) \\ = \text{CA Measurement area } (i) \cup \text{CA Measurement area } (i + 1) \end{aligned} \quad (1)$$

For example, the contact angle data used to characterize the surface of testing sample number 1 ($i = 1$), includes the contact angle data of both CA measurement areas number 1 (i) and 2 ($i + 1 = 2$). In the case of testing sample number 2, the contact angle that characterizes it is comprised of CA measurement area numbers 2 and 3.

When measuring the CA, marks are done every inch on each laminate of SLS and DSJ batches to identify the different CA measurement areas as seen in Figure 19. This method assures that it is possible to correlate later the registered CA data with the later mechanical testing results of each sample.

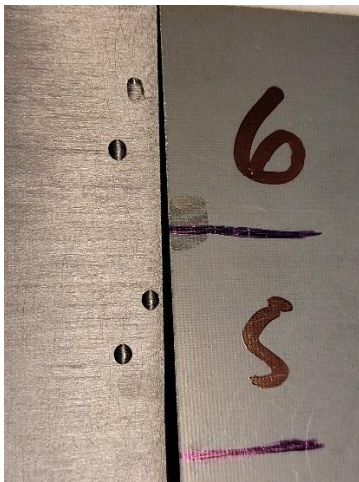


Figure 19: Water drops left on the surface of the laminate after CA measuring

Once the CA has been measured on a laminate, the water drops are left to dry in the laboratory environment. This drying process should not take more than 15 minutes.

5.6 Manufacturing

Even though the manufacturing of the SLS and DSJ batches is not identical, they share several common elements. For example, they share the same preparation steps, such as removing the FM 300-2 from storage and putting it at room temperature, where it should stay for at least 2 hours before opening the package containing it. Another preparation step is to bring the materials necessary to make the vacuum bag to the laboratory and to check that the recording software of the thermocouples is working properly, providing correct temperature readings. If not used for some weeks, a small test in the oven is performed at constant temperature to check that the thermocouples temperature readings are matching the ones obtained from the oven.

After all the preparation steps, one of the surface treatments already described in Chapter 5.4 is applied to the laminates that are going to be bonded. Once the surface treatment has been completed, the CA measurement procedure described in Chapter 5.5 is carried out. Then, the adhesive is cut using metallic scissors and a calliper to obtain the necessary adhesive dimensions, which depend on the type of adhesive joint being manufactured as seen previously in Chapter 5.3. Once the adhesive is cut, the FM 300-2 is placed between the laminates (Figure 20) and the different parts of the samples are assembled with the help of the manufacturing tools described previously in Chapter 5.2. This step and the materials used on it are the main difference between SLS and DSJ manufacturing. The assembly of DSJ samples is significantly more complex due to the higher number of components needed to produce this type of adhesive joint and the necessary cutting of a Teflon stripe and 2 straps from a type-B laminate.

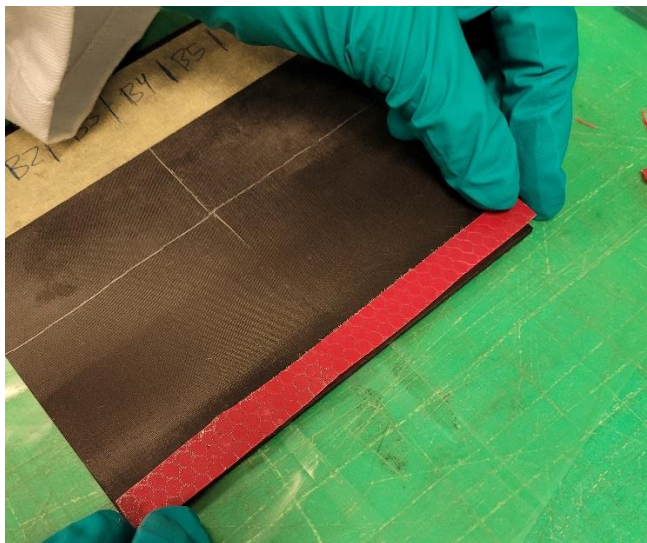


Figure 20: Placing of FM 300-2 sheet on a type-A laminate while manufacturing a SLS sample

After assembling correctly the manufacturing batch, 1 or 2 thermocouples are attached on the laminate's external surface closest to the bonding area. Then, a vacuum bag envelope is created around the batch. First, the vacuum film is put on a working table. Then, sealing tape is added on its edges. After that, the batch is put over the vacuum film and covered completely by the "Teflon" envelope and later by the "cotton" envelope. These 2 envelopes should have a small cut to let the thermocouples cables connect the batch to the outside. Finally, the vacuum tube coming from the pump is added and the top-vacuum film is put on top of everything, covering and sealing the vacuum bag thanks to the sealing tape. Once sealed, the vacuum pump is turned on and the vacuum bag sealing is inspected and improved by gently tapping with the fingers over the areas where some air channels are detected.



Figure 21: Vacuum bag inside the oven with thermocouples and vacuum ready for curing process

Then, the thermocouple software starts recording the temperature and the vacuum bag with the sample inside is put in the oven as seen in Figure 21. The oven should be at room temperature. The curing process is done inside the oven at 120 °C for 2 hours while applying a vacuum of 0.7 bar with the vacuum pump. The heating ramp to reach the curing temperature of 120 °C is done at 2 °C/min. The temperature-time diagram of the curing process is presented in Figure 22. Once the curing is finished, the oven is turned off and it is slightly opened to cool down until reaching ambient temperature. During the cooling down the pump is not turned off, to ensure that the process is as smooth as possible. After the cooling down, the thermocouple recording software is stopped, the vacuum bag is removed from the oven and the batch is extracted from it.

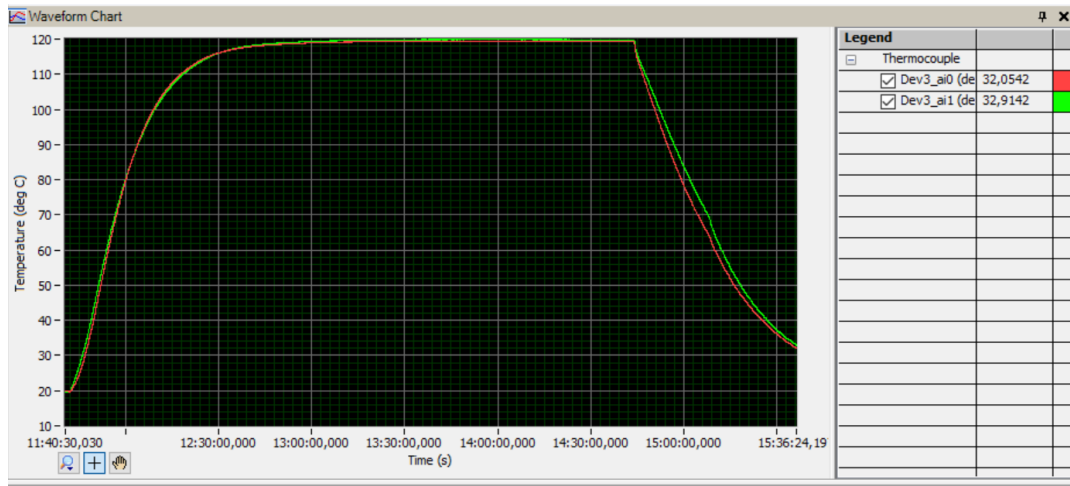


Figure 22: Temperature-time diagram of the FM 300-2 curing cycle obtained using 2 thermocouples

The last step in manufacturing is water-jet cutting the manufactured 6"-wide SLS and DSJ batches into 5 smaller 1"-wide pieces to meet with the established dimensions in Chapter 5.3. This cutting process is outsourced to a specialized cutting company. After obtaining the cut-pieces, they are measured individually as the following schematic of Figure 23 presents. The thickness and width are measured at each numbered point. The length of each sample is also measured. These measurements are necessary to estimate the bonding width of each sample and to check that differences in thickness and length are kept minimal.

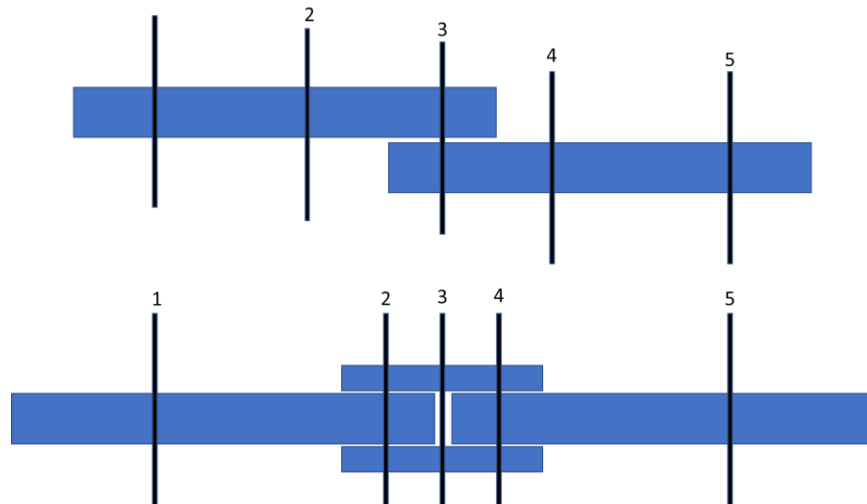


Figure 23: Schematic with measurement points of SLS (top) and DSJ (bottom) samples

End-tabbing of SLS samples can be performed either before or after water-jet cutting the samples, but performing it before the water-jet cutting makes the process simpler. To produce the tabbing plates it is necessary to cut a type-A laminate with a cutting machine. Once the tabbing plates are ready, their peel ply is removed and they are sanded to a

light sanding level. The areas of the laminates where the tabbing plates are going to be glued are also roughened. After sanding, the dust is cleaned and Araldite glue is applied on the tabbing plates with a glue gun and distributed evenly on all their bonding surface. Then, the tabbing plates are glued to the laminates and some pressure is put on them for the whole curing process to ensure that the bonding is correct. After the 24-hour curing process, the end-tabbed SLS batches are ready to be water-jet cut.

5.7 Environmental exposition after bonding

Finished adhesive joints were exposed to an ETW environment to understand how it affects the bonding strength of the different surface treatments, as well as to compare the bonding strength obtained with ETW environment to the strength obtained at RTA conditions. The ETW environment characteristics were 60 °C temperature and 95% relative humidity, and they were obtained inside the environmental chamber (Figure 24). The samples were kept in this ETW environment for 15 days and they were immediately tested after that period to prevent moisture loss and minimize temperature reduction. Only 2 types of samples (and surface treatments) were exposed to this environment: SLS with Baseline treatment and SLS with Grease contamination. The weight of the samples exposed to the ETW environment was recorded periodically to measure their moisture absorption.



Figure 24: SLS Grease ETW samples inside the environmental chamber

5.8 Mechanical testing

All the mechanical testing at ambient environment is conducted in an Instron electric load cell with a maximum load capacity of 30 kN. Samples are left on the testing ambient environment for at least 24 hours to stabilize them before the testing. The temperature of the RTA testing environment ranges from 22 to 24 °C, and the RH is between 50 and 55%. For the samples that have been exposed to the ETW environment the same testing cell is used, but they are kept inside closed plastic bags and warmed up to 60 °C inside an oven before testing. The high temperature of the samples when compared with the environment was captured with the FLUKE thermal imager presented in Figure 25. It should be noted that the temperature values obtained with the reader were only qualitative, since the emissivity of the CFRP samples was not considered.



a) FLUKE thermal imager used



b) Qualitative temperature reading of ETW sample during testing with same thermal imager

Figure 25: Thermal imager and thermal image obtained during ETW testing

Other than the environment differences, the testing of SLS and DSJ samples is identical and quite straightforward: first, the samples are mechanically clamped to the load cell with a clamping length of 1", as seen in Figure 26.

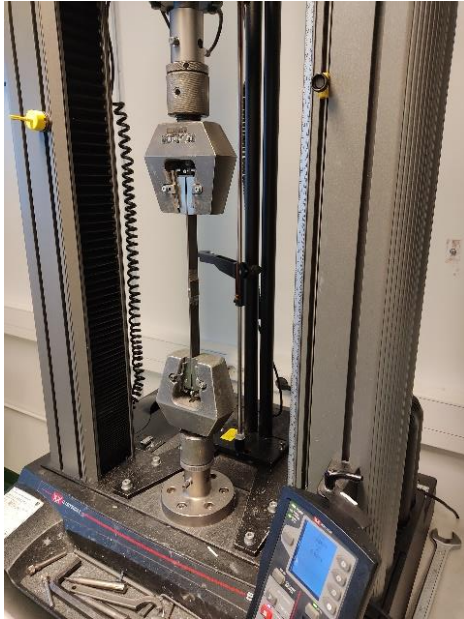


Figure 26: DSJ sample clamped to the load cell just before testing

Then, a positive extension rate of 2 mm/min is applied to them until their adhesive bond is broken, resulting in a heavy load drop in the load cell. The maximum load recorded during testing is saved, as well as the load-extension curve of each sample. Additionally, pictures of the different failure surfaces are taken for later analysis and comparison.

6. RESULTS & ANALYSIS

6.1 Contact angle results

In this chapter the average (avg.) contact angle as well as the maximum (max.) and minimum (min.) measured contact angle values of each surface treatment and type of sample are presented. Additionally, the standard deviation (SD) is also calculated. The standard deviation provides an idea of how the values are distributed: a higher SD means that the values are quite spread, whereas a low SD means that the values are mostly distributed close to the average CA value.

The average, maximum and minimum CA of each surface treatment applied in SLS samples is presented in Figure 27. The SD of each surface treatment is also presented in the figure as an error bar in the average CA. About the nomenclature used, it should be noted that Baseline* includes the CA data of both Baseline and Baseline (ETW). Similarly, Grease* results correspond to the CA data of both Grease and Grease (ETW).

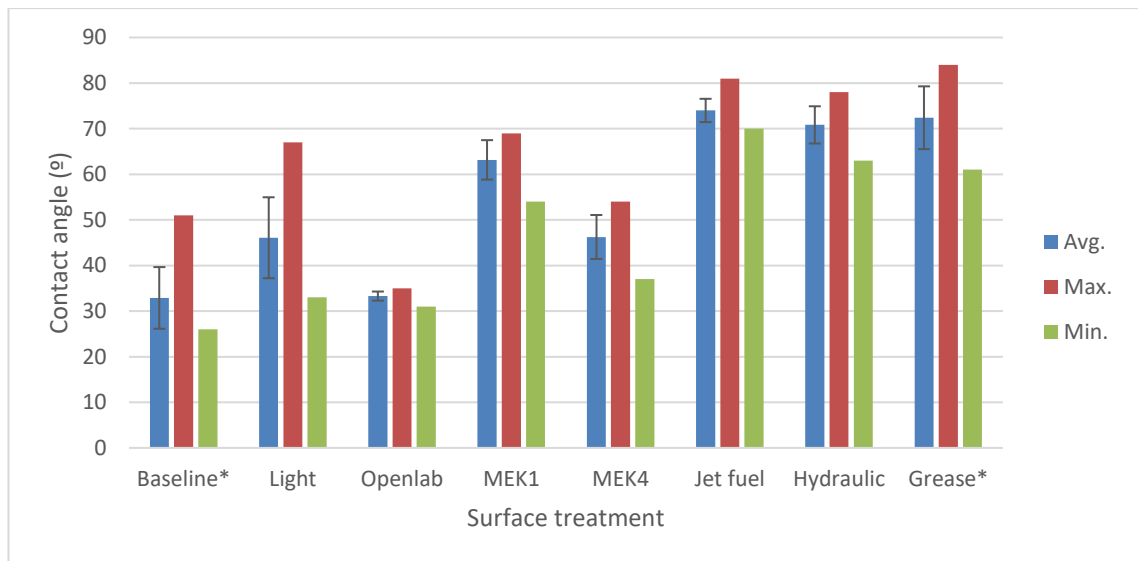


Figure 27: Average, maximum and minimum CA per surface treatment in SLS samples. SD is plotted as error bar in the average CA

The highest CA values in SLS samples were reached with the contamination treatments, i.e., Grease, Jet fuel and Hydraulic fluid contamination treatments. The lowest CA values were obtained with Openlab contamination and Baseline* treatments. In terms of SD and maximum-minimum CA difference, Baseline* and Light sanding were the ones with the highest values. This was especially true in the case of Light sanding, where not just the SD was high, but the difference between the maximum-minimum CA difference was 34°,

which is equivalent to the 74% of the average CA of Light sanding. MEK-cleaning treatments presented higher average CA than Baseline*, which could be an indication that some MEK remained in the bond surface. MEK1 presented higher CA values than MEK4 treatment.

The following Figure 28 presents the same CA parameters as Figure 27 but applied to DSJ samples and their surface treatments.

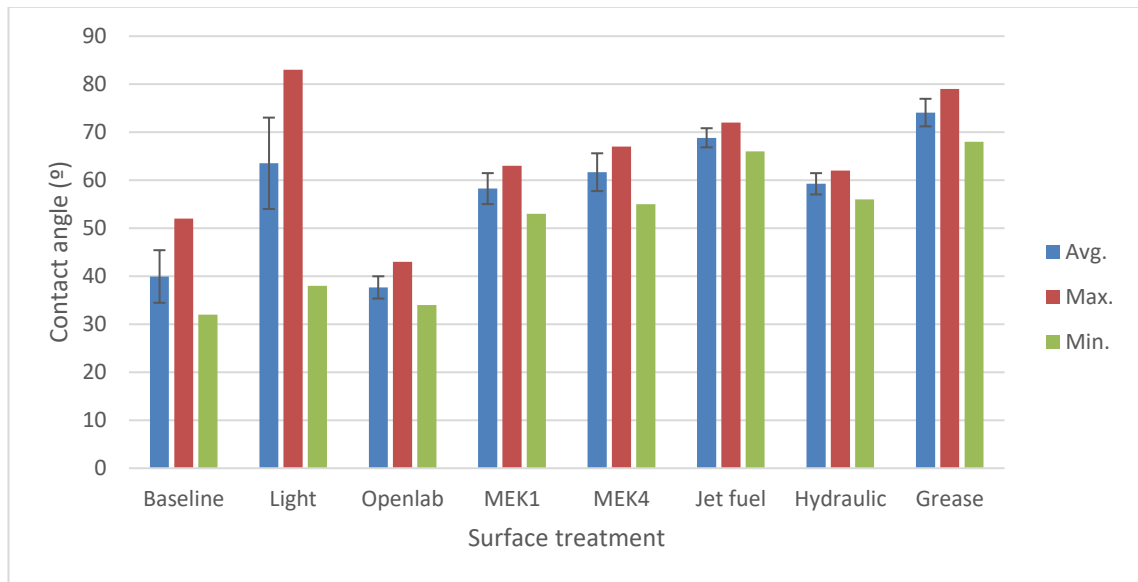


Figure 28: Average, maximum and minimum CA per surface treatment in DSJ samples. SD is plotted as error bar in the average CA

The CA results of DSJ samples followed the same main trends as the SLS ones: Grease, Jet fuel and Hydraulic fluid contamination treatments presented the highest average CA, while Openlab and Baseline treatments had the lowest average CA values. Additionally, the highest data spread was also obtained in the Light sanding treatment. Nonetheless, the CA of MEK-cleaning treatments seem to be higher than the ones from SLS samples. Additionally, MEK4 had a higher average CA than MEK1, unlike in the case of SLS samples. To obtain a better comparison, the average CA of each surface treatment and their corresponding SD in both SLS and DSJ samples are plotted in the following Figure 29.

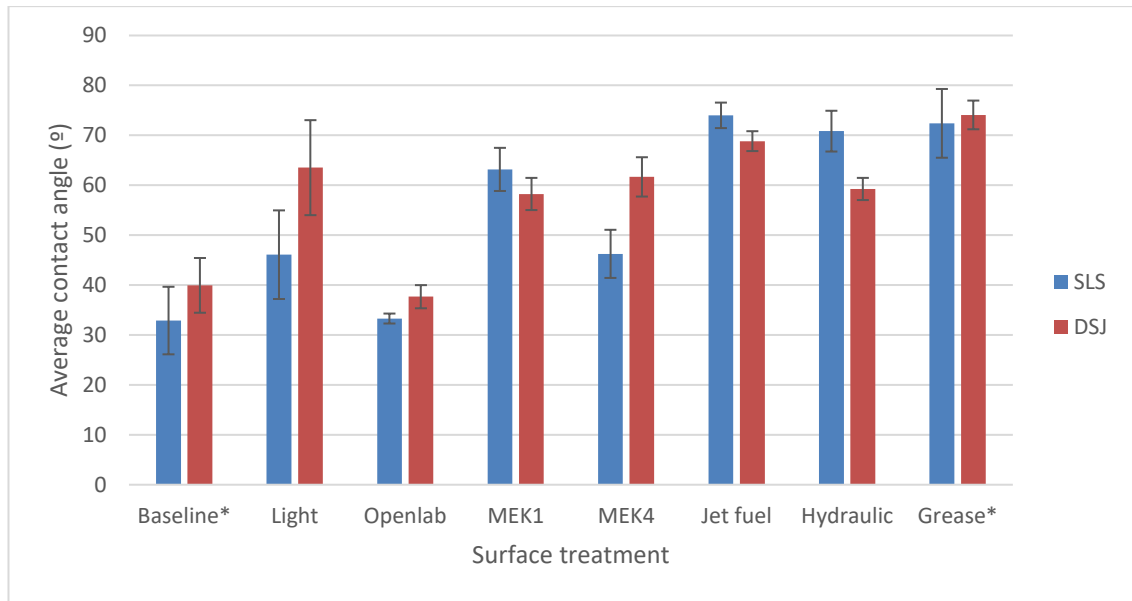


Figure 29: Comparison of average CA and SD between SLS and DSJ samples

Theoretically, the CA values of the surface treatments presented in Figure 29 should be the same in SLS and DSJ samples, since the same procedure was followed in both types of samples. In fact, the CA values of some surface treatments were almost the same in both types of samples. This is the case of Openlab, MEK1, Jet fuel and Grease treatments, where only minor differences (less than 12%) are appreciated in average CA. Additionally, the small differences in average CA do not follow a clear trend: the average CA of Openlab and Grease treatments was higher in DSJ samples, whereas the average CA of MEK1 and Jet fuel treatments was higher in SLS samples.

On the other hand, the remaining surface treatments (Baseline, Light sanding, MEK4 and Hydraulic fluid) showed quite different CA results in SLS and DSJ samples. For example, the average CA of MEK4 in DSJ samples is almost a 30% higher than the average CA in SLS ones.

These substantial differences in CA between types of samples for the same surface treatment could be due to environmental factors such as temperature and humidity during CA measuring (which were not controlled), as well as the occasional presence of dust or other solid particles in suspension that could have deposited on the surface during the 15-minute dwell time. Additionally, some human-factors that could have contributed to this CA difference are variations in sanding depth and pattern, resulting in variation of the surface roughness. Moreover, other human-induced factors to consider are differences in the amount of contamination deposited on the surface, as well as differences in the cleaning processes and in the use of MEK in the corresponding treatments.

Finally, the SD of the surface treatments changed significantly from SLS to DSJ samples. For example, in the case of Grease, its SD in DSJ samples was more than double than the SD obtained in SLS ones. SD differences between SLS and DSJ samples could be attributed to the same factors already described as possible reasons behind average CA differences.

6.2 Mechanical testing results

During mechanical testing the maximum force of each individual sample is recorded. To take into account the effect of the possible geometry variations between the samples, the maximum force obtained during testing is divided by the bond area of each sample, as seen in Equation (2), obtaining the maximum joint stress of each sample. The bond area of SLS joints is calculated with Equation (3) and the bond area of DSJ is calculated with Equation (4). The bond length in SLS joints is considered as 0.5" whereas in DSJ samples it is considered as 1". On the other hand, the bond width of both types of samples is obtained from measuring each sample.

$$\text{Maximum joint strength} = \frac{\text{Maximum force}}{\text{Bond area}} \quad (2)$$

$$\text{Bond Area}_{SLS} = \text{Bond length (0.5")} \cdot \text{Bond width (measured value)} \quad (3)$$

$$\text{Bond Area}_{DSJ} = \text{Bond length (1")} \cdot \text{Bond width (measured value)} \quad (4)$$

The results of applying the previous equations and calculating the maximum shear stresses are presented in Table 6 and Figure 30. Before discussing the results, it should be noted that the strength results obtained with DSJ are considered more relevant than the ones obtained with SLS joints, since they characterize better the shear behaviour of the adhesive-adherends due to their significantly lower peel forces and eccentricity. Nonetheless, SLS testing is more widespread due to their easier manufacturing, and that is why it is also performed.

Table 6: Average maximum stress and standard deviation per surface treatment and sample type

Surface treatment	DSJ Max. Stress (MPa) (Avg. ± SD)	SLS Max. Stress (MPa) (Avg. ± SD)
Baseline	39.9 ± 4.2	30.5 ± 1.8

Light sanding	37.4 ± 3.3	28.7 ± 1.2
Openlab	38.8 ± 5.0	45.0 ± 2.9
MEK1	27.8 ± 2.4	47.6 ± 2.7
MEK4	28.2 ± 1.1	47.0 ± 1.7
Jet fuel	28.2 ± 1.1	45.4 ± 2.7
Hydraulic fluid	30.6 ± 1.7	44.9 ± 1.9
Grease	25.9 ± 1.6	37.7 ± 4.0

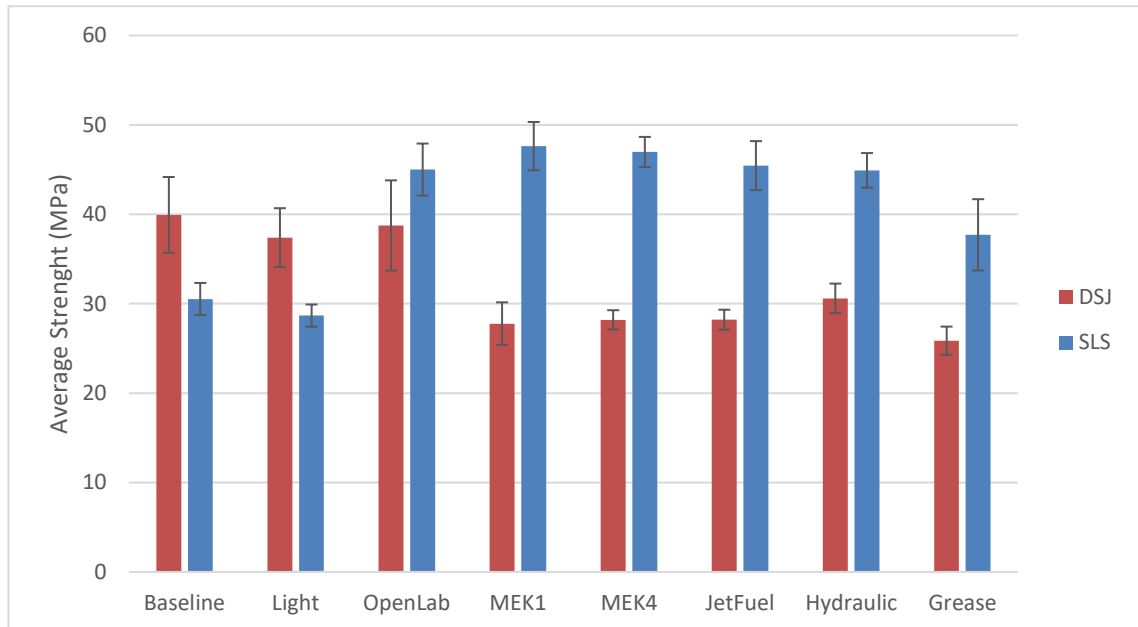


Figure 30: Comparison of the maximum average stress and SD between SLS and DSJ samples

As seen in both Table 6 and Figure 30, the maximum average strength in DSJ samples was obtained with Baseline treatment, followed closely by Openlab and Light sanding. MEK-cleaning and Jet fuel, Hydraulic fluid and Grease contamination treatments obtained quite similar strength results to each other, but their strength was low when compared with Baseline, Openlab and Light sanding. Based on these mechanical testing results, it seems like wiping the surface with a dry cloth after sanding led to a higher bond strength than using MEK to clean the surface. Moreover, these results show that cleaning the surface with MEK had a similar negative impact on the bond strength as contaminating the surface with agents like jet fuel, hydraulic fluid or grease.

In the case of SLS samples, the results were quite different. The highest bond strength was obtained with MEK1 and MEK4 cleaning treatments, followed closely by Jet fuel, Hydraulic fluid, and Openlab contamination treatments. Moreover, Light sanding and Baseline treatments presented the lowest strength values from all the tested SLS samples. The strength of Grease contamination treatment was lower than the previously mentioned MEK-cleaning and contamination treatments, but it was still substantially higher than the bond strength of Baseline and Light sanding treatments. MEK1

In order to visualize better the average strength of each surface treatment in both DSJ and SLS samples, the average strength of each surface treatment was divided by the maximum strength of the corresponding joint type (i.e., by the maximum strength of DSJ or SLS samples), obtaining as a result a strength ratio. The results of this relativization exercise are plotted as relative percentages of the maximum joint strength (or strength ratio) in Figure 31.

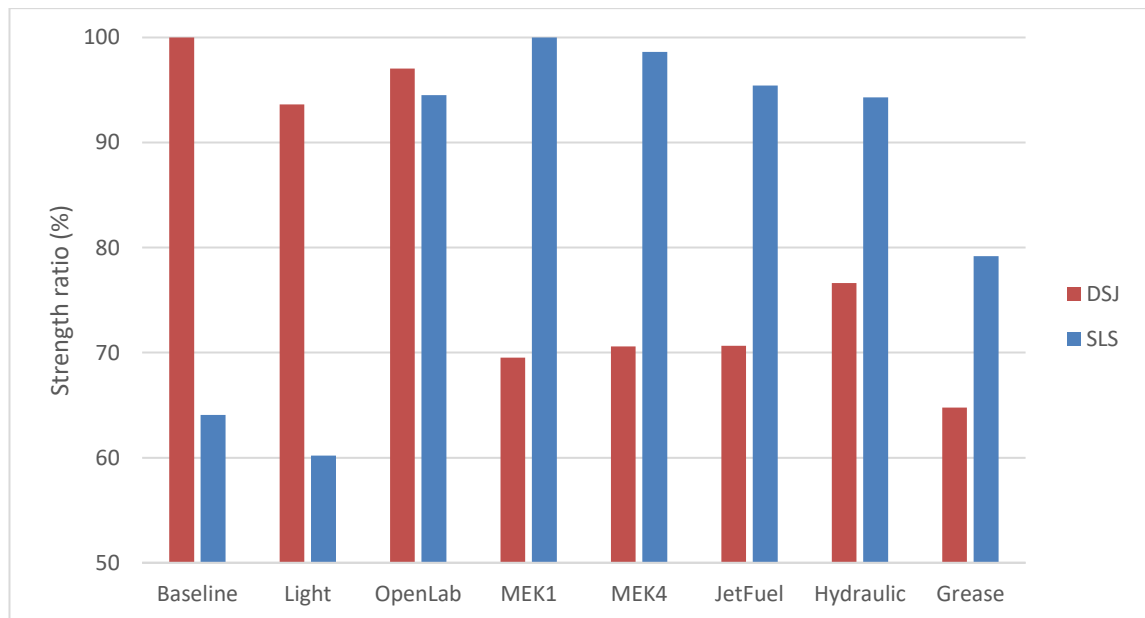


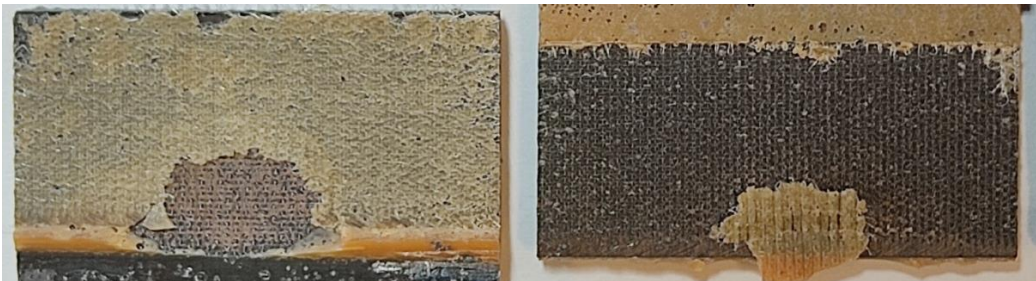
Figure 31: Normalized strength comparison of DSJ and SLS surface treatments using the strength ratio

As seen in Figure 31, Light sanding and Baseline treatments had a far higher strength ratio in DSJ samples than in SLS samples. On the other hand, MEK-cleaning treatments and all contamination treatments (except Openlab) obtained significantly lower strength ratios in DSJ. For example, MEK1 had the lowest strength in DSJ but the highest strength ratio in SLS samples. Openlab contamination treatment had the most stable strength ratio in SLS and DSJ, only experiencing a 2% increase from SLS joints to DSJ. The strength ratio differences could be explained with the different loading modes that the joints experience in each case: the loading in DSJ is almost 100% shear, whereas in

SLS joints peel forces are significant and could have influenced the strength results. Nevertheless, it should be noted that all the tested SLS and DSJ samples but 2 performed above the commonly established 25 MPa lower limit for joints made with FM 300-2 adhesive [45]. The exceptions were one DSJ Grease and another DSJ MEK1 sample, whose strength was 24.8 and 24.4 MPa, respectively.

6.3 Failure surfaces analysis

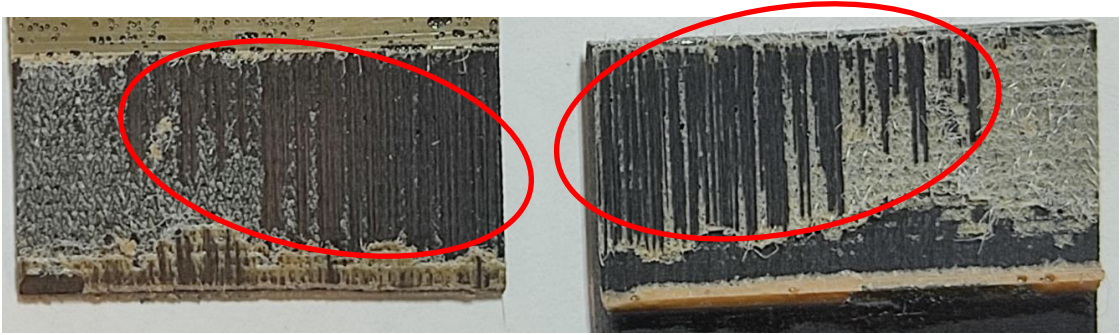
Studying the failure surfaces and the failure modes on them is necessary to understand better the strength results obtained from testing. In this chapter the failure surfaces of both SLS and DSJ samples are classified according to the ASTM D5573 standard already described in Chapter 4.6. The main 4 failure modes observed in the tested samples are adhesive failure, cohesive failure, light fibre-tear failure and fibre-tear failure. A visual example of each one of these failure modes is presented in the following Figure 32. Due to their very similar morphology, light-fibre tear and fibre tear failures are both categorized as delamination failure mode in this chapter. Additionally, it should be noted that due to the epoxy nature of the adhesive (FM 300-2) and the epoxy matrix of the adherends it is not easy to identify a clear adhesive failure as described in ASTM D5573 standard.



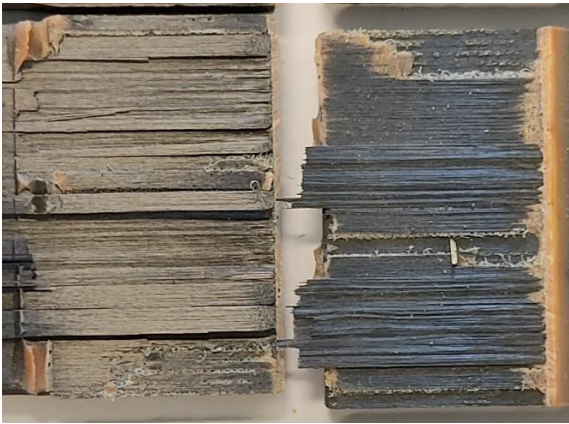
a) Adhesive failure (DSJ Light, sample 5, G&H interface)



b) Cohesive failure (DSJ Jet fuel, sample 5, F&E interface)



c) Light-fibre tear failure (DSJ Baseline, sample 2, F&E interface)



d) Fibre tear failure (SLS Openlab, sample 3)

Figure 32: Representative surfaces of main failure modes

Due to the large amount of fracture surfaces of SLS samples, only one failure surface of each surface treatment is presented in the following Figure 33 and the average failure mode of each surface treatment in SLS samples is presented in Figure 34. The failure pictures have been chosen with the aim of representing the average failure surface of each surface treatment as accurately as possible.



a) Baseline (sample 8)



b) Light sanding (sample 1)



c) Openlab (sample 3)



d) MEK1 (sample 1)



e) MEK4 (sample 1)



f) Jet fuel (sample 1)



g) Hydraulic fluid (sample 5)



h) Grease (sample 4)

Figure 33: Representative failure surfaces of each surface treatment applied to SLS samples

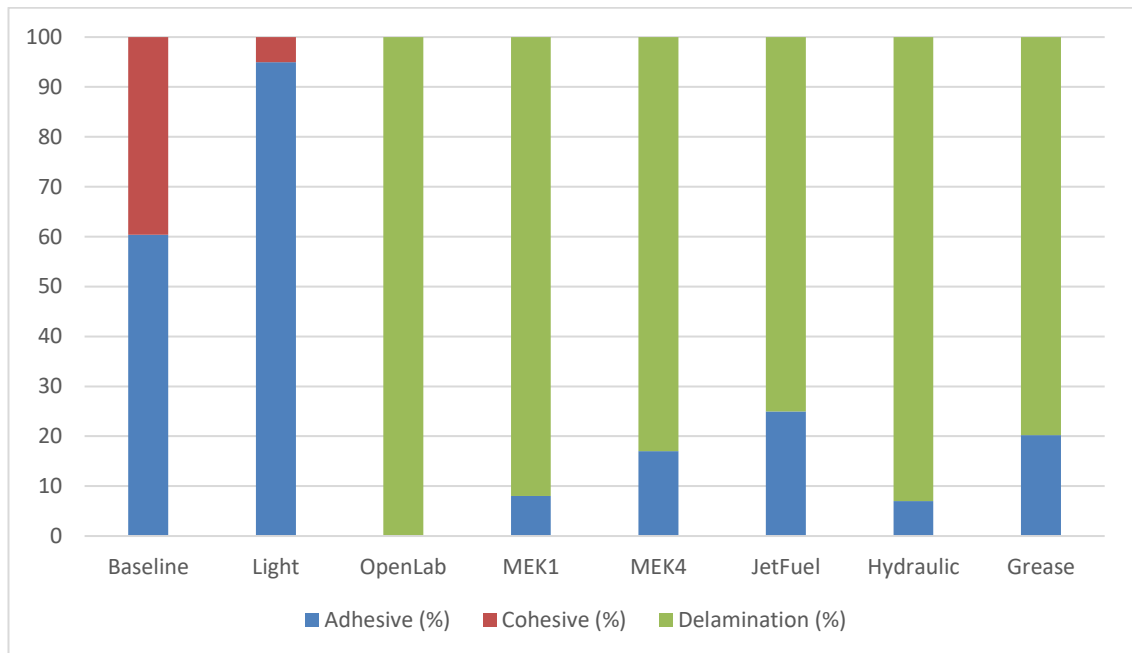
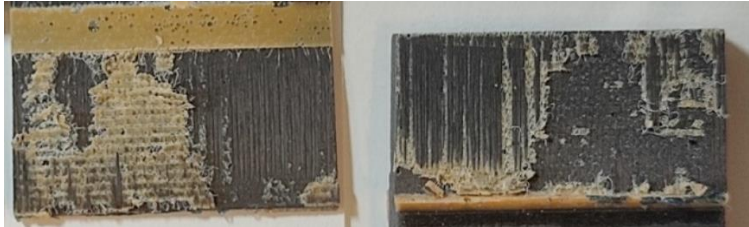


Figure 34: Average failure mode in SLS samples

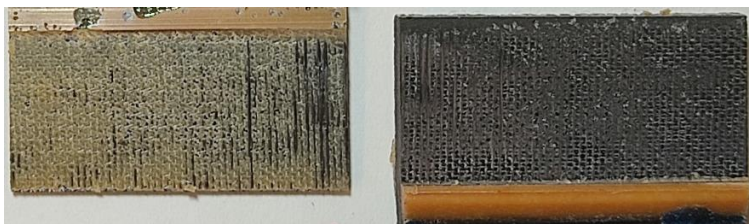
Based on the results presented in Figure 34 as well as the failure surfaces of Figure 33, adhesive failure represented the main failure mode in 60% of Baseline surfaces and in almost 100% surfaces of Light sanding. Baseline had a significant higher cohesive failure mode than Light sanding, which could be related to its higher joint strength. The main failure mode in all the contaminated surfaces and the MEK-cleaned ones was delamination (80-100%), followed by adhesive failure. No clear cohesive failure could be identified in any of their surfaces. Thus, both surface contamination treatments and MEK-cleaning treatments increased significantly the presence of delamination failure mode when compared to surfaces which were only sanded and cleaned with dry-cloth. These failure mode results mean that SLS treatments can be divided in 2 groups: adhesive failure group and delamination group. The adhesive group includes the surface treatments whose main failure mode was adhesive failure, whereas the surface treatments inside the delamination group are the ones whose main failure mode was delamination. Baseline and Light sanding treatments belong to the first group, whereas MEK-cleaning and all contamination treatments belong to the delamination group. The significant difference in failure mode between these 2 groups could be the one of the reasons why their mechanical testing results were so different.

In the case of DSJ, the failure mode analysis of each surface treatment is more complex, since only half of the interfaces were contaminated (or cleaned) in most of them. Because of that, it is necessary to distinguish between the contaminated interfaces and the

non-contaminated ones. This does not apply to Baseline, Light sanding and Openlab treatments, because these surface treatments were applied to all DSJ bonding interfaces. First, representative images of each surface treatment's contaminated failure surfaces is presented in Figure 35. Then, the average failure mode in the DSJ contaminated interfaces is presented in Figure 36.



a) Baseline (sample 4, interface E&F)



b) Light (sample 3, interface E&F)



c) Openlab (sample 2, interface C&D)



d) MEK1 (sample 4, interface G&H)



e) MEK4 (sample 2, interface G&H)



f) Jet fuel (sample 4, interface E&F)



g) Hydraulic fluid (sample 4, interface G&H)



h) Grease (sample 3, interface G&H)

Figure 35: Representative failure surfaces of each surface treatment applied to DSJ samples

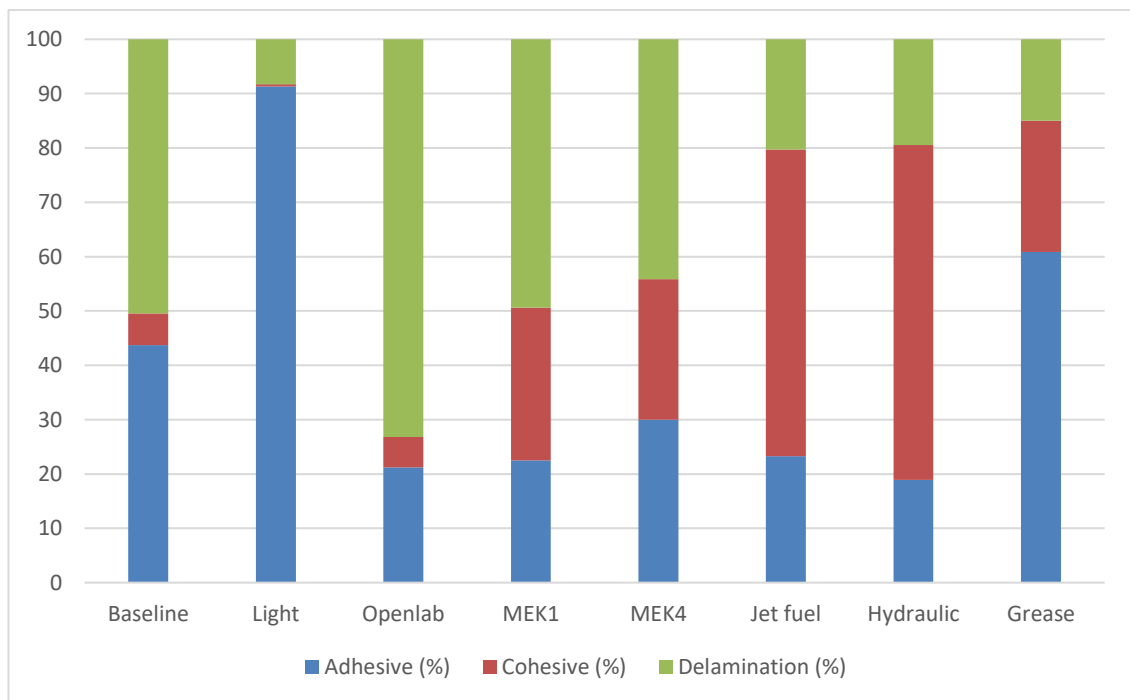


Figure 36: Average failure mode in contaminated DSJ interfaces

As in the case of SLS, Light sanding was the surface treatment with the highest adhesive failure. But unlike in SLS, Grease samples were the ones with the second-highest adhesive failure. Baseline had also a high adhesive failure, but delamination represented 50%

of all its failure surfaces, unlike in SLS, where no delamination was observed at all. Overall, there were failure surfaces with cohesive failure in DSJ than in SLS samples. For example, cohesive failure represented the main failure mode of Jet fuel and Hydraulic fluid. Nonetheless, it is interesting to note that Baseline, Light sanding and Openlab treatments had the lowest percentage of cohesive failure but the highest strength during testing.

To assess better the influence of the contamination and cleaning treatments, the failure mode of the DSJ contaminated interfaces is compared with their non-contaminated interfaces, which only received a baseline treatment. This comparison is performed in Figure 37. Contaminated interfaces are marked with “-C” and the non-contaminated ones are marked with a corresponding “-NC”.

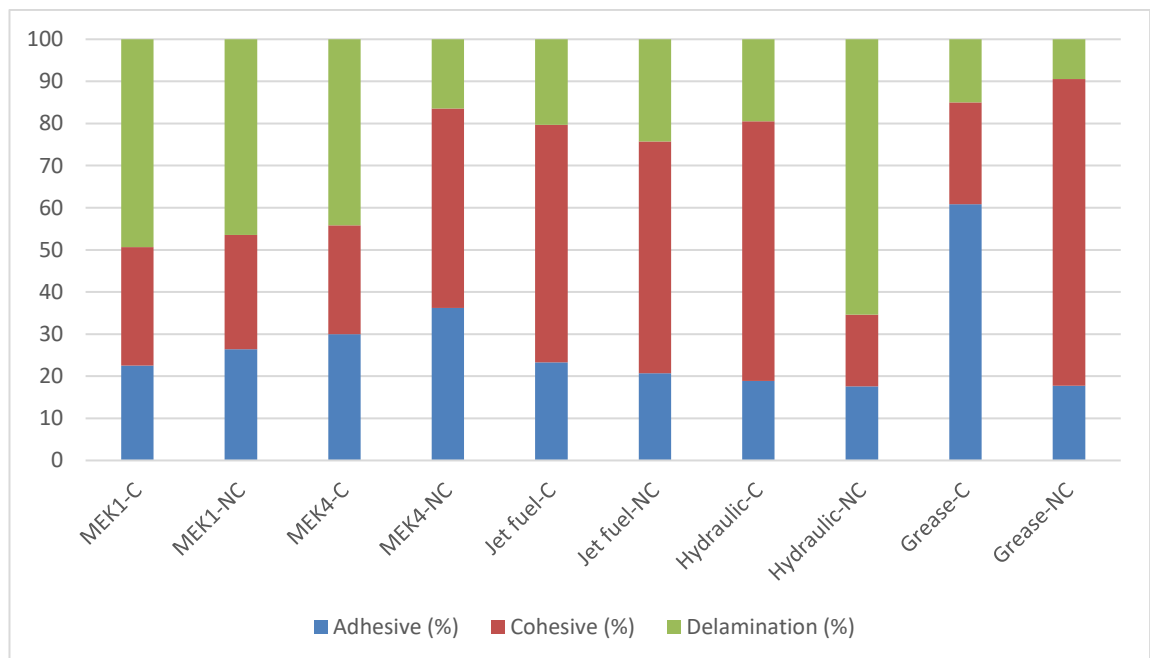


Figure 37: Side-by-side comparison of average failure mode in contaminated (C) and non-contaminated (NC) DSJ interfaces

As seen in Figure 37, not all the surface treatments obtained the same failure results in the contaminated and in non-contaminated interfaces. For example, delamination had a 65% weight in the non-contaminated interfaces of hydraulic fluid samples but only represented 20% of the contaminated interfaces. MEK4 had higher delamination and Grease had higher adhesive failure in the contaminated interfaces, but both had a significantly higher cohesive failure mode in the non-contaminated interfaces. The exceptions were MEK1 and Jet fuel treatments, which presented surprisingly almost the same average failure mode in both contaminated and not-contaminated interfaces.

6.4 Contact angle – bonding strength correlation

In this chapter the contact angle and the bonding strength of each sample tested is plotted with the aim of understanding if there is a correlation between these 2 parameters: the surface contact angle and the bond strength. To make the study deeper, the average, the maximum and the minimum contact angle obtained from each individual testing sample are plotted against the maximum average stress registered in each sample during their testing.

As stated previously, testing of DSJ samples is more reliable and representative of adhesive-adherends shear behaviour than testing of SLS joints. Because of that, DSJ results are also considered the most relevant ones for the CA-bond strength correlation, and they are the first ones to be presented. Figure 38, 39 and 40 plot the joint strength of each sample against its corresponding average, maximum and minimum contact angle, respectively. Linear trend lines are also plotted for each graph, as well as their coefficient of determination (R^2), which quantifies how well does the data fits the linear correlation plotted in the graph. The closer R^2 is to 1, the better linear correlation is obtained.

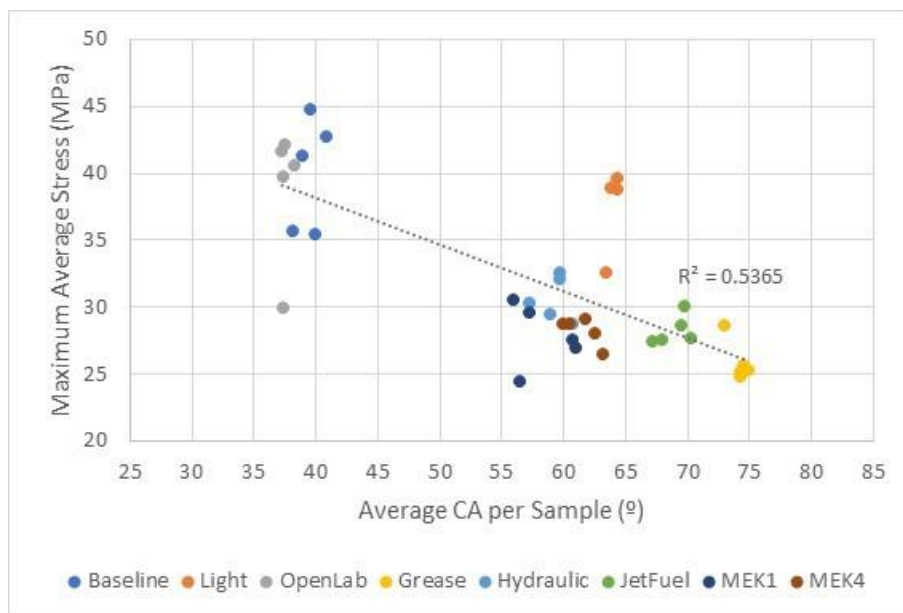


Figure 38: Joint strength - Average CA comparison of DSJ samples

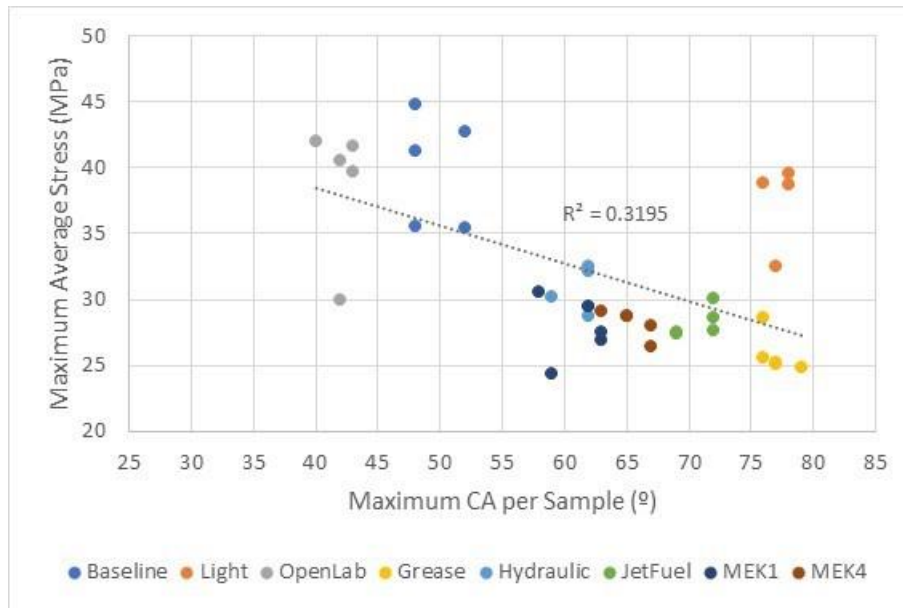


Figure 39: Joint strength - Maximum CA comparison of DSJ samples

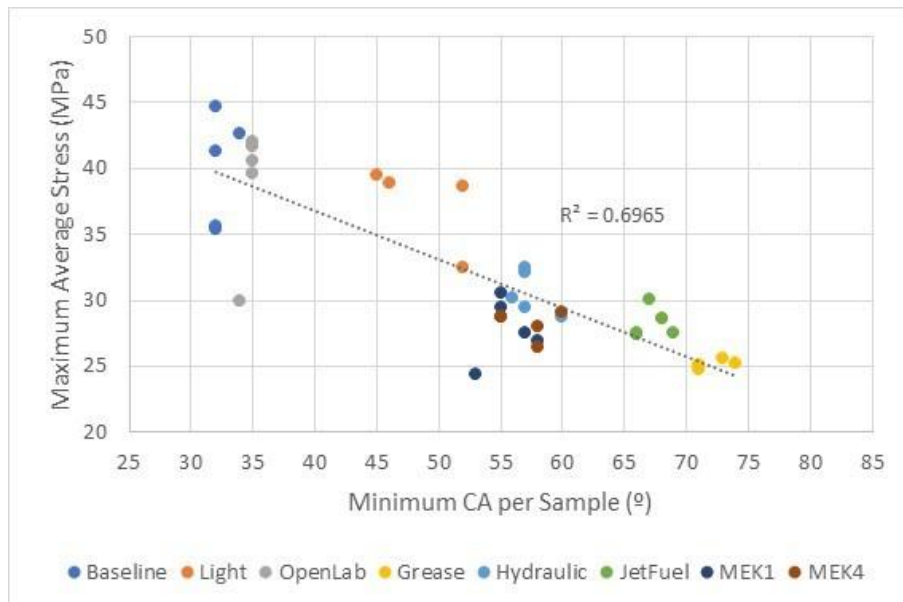


Figure 40: Joint strength – Minimum CA comparison of DSJ samples

Observing the CA-strength plots, the strongest CA-strength correlation is obtained with the minimum CA ($R^2 = 0.70$) and the average CA ($R^2 = 0.54$). The maximum CA-strength correlation is the weakest, with a mere ($R^2 = 0.32$).

Focusing on Figure 40 results, a clear trend is visible between low minimum CA and high bond strength (e.g., in Baseline and Openlab batches) as well as between high minimum CA and low bond strength, since the 2 surface treatments with the highest minimum CA (Grease and Jet fuel contamination treatments) are the ones with the lowest bond strength. Nonetheless, the CA-strength correlation is not as straightforward in the re-

maining surface treatments. Baseline and Openlab treatments provide quite similar minimum CA and strength values, almost overlapping, although the CA data of the Openlab samples is far more uniform. Hydraulic fluid contamination and MEK-cleaning treatments minimum CA and strength values seem to be quite similar to each other, even partially overlapping some data points. Based on average, maximum and minimum CA results obtained, it should be easy to identify different types of sanding just by measuring the CA. For example, the Light sanding sample with the lowest average CA is still 23° higher than the lowest average CA found in any Baseline sample. Even with this considerable CA difference, the bond strength results do not differ greatly between both types of sanding. The same could be said for the contamination treatments (except Openlab) and MEK-cleaning treatments, which have more than 20° higher average CA than Baseline treatment.

Nevertheless, in order to confirm or reject the CA-strength correlation obtained with the DSJ data it would be necessary to analyse the influence of the failure mode in the strength of each sample, since delamination was the main failure mode of Openlab, Baseline, MEK1 and MEK4 treatments, cohesive failure was the main one of Jet fuel and Hydraulic fluid contamination treatments and adhesive failure was the main failure mode of both Light sanding and Grease treatments.

In the case of SLS results, Figure 41, 42 and 43 plot the joint strength of each sample against its average, maximum and minimum contact angle, just like previously done with DSJ. The trend lines plotted on these figures are also linear.

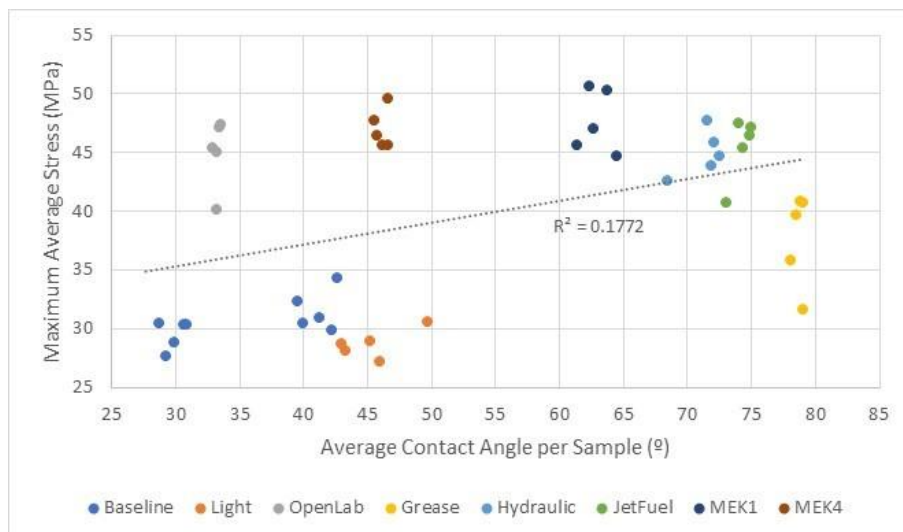


Figure 41: Joint strength – Average CA comparison of SLS samples

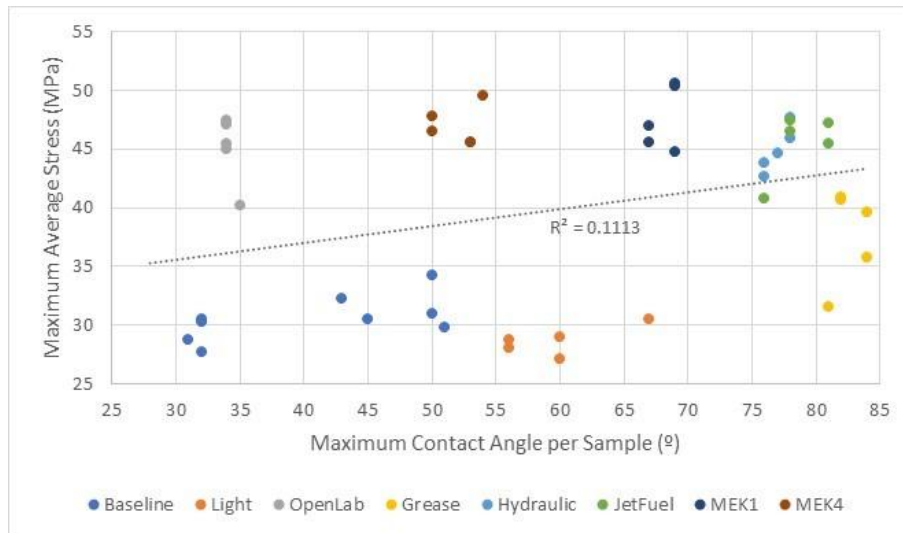


Figure 42: Joint strength – Maximum CA comparison of SLS samples

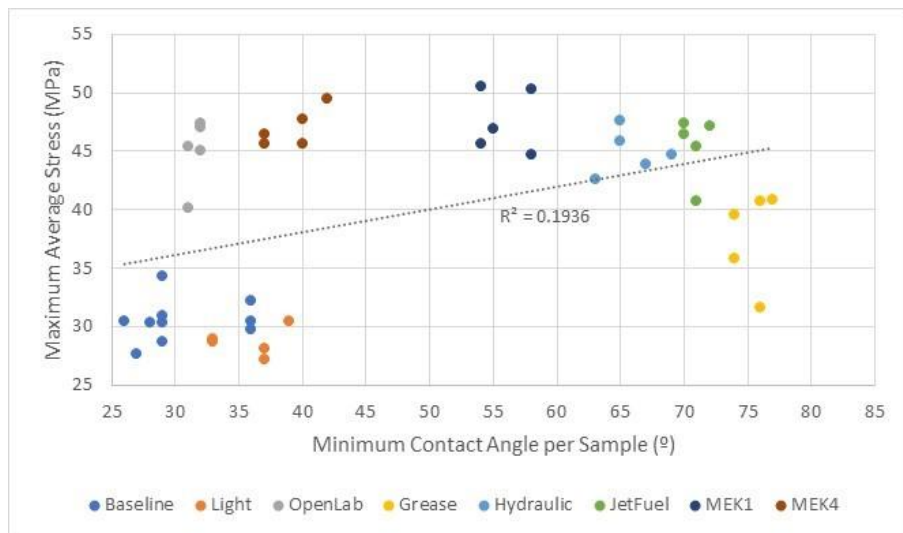


Figure 43: Joint strength – Minimum CA comparison of SLS samples

As can be seen in all the previous plots for SLS samples, the coefficient of determination of all the trend lines is quite low, below 0.2. These low coefficients of determination mean that, with the present data, it is not possible to obtain a clear CA-strength correlation in SLS samples. Nevertheless, just like in DSJ, a further analysis should be performed to study the influence of the main failure mode of each SLS sample on the obtained strength. For example, as previously presented in Figure 34, the main failure mode of all the contamination and MEK-cleaning treatments in SLS joints had a far higher delamination failure in their surfaces than Baseline and Light sanding samples, and they also had a far higher bond strength.

6.5 Environmental exposition results

The CA results of the ETW treated samples (SLS Baseline ETW and SLS Grease ETW) were very similar to their RTA counterparts, as they should, since they received the same surface treatment: Grease samples presented a far higher CA than Baseline ones. The CA data is available in Appendix A. The strength of the samples exposed to the ETW environment is compared with the strength of the ones that were only exposed to RTA environment in Figure 44.

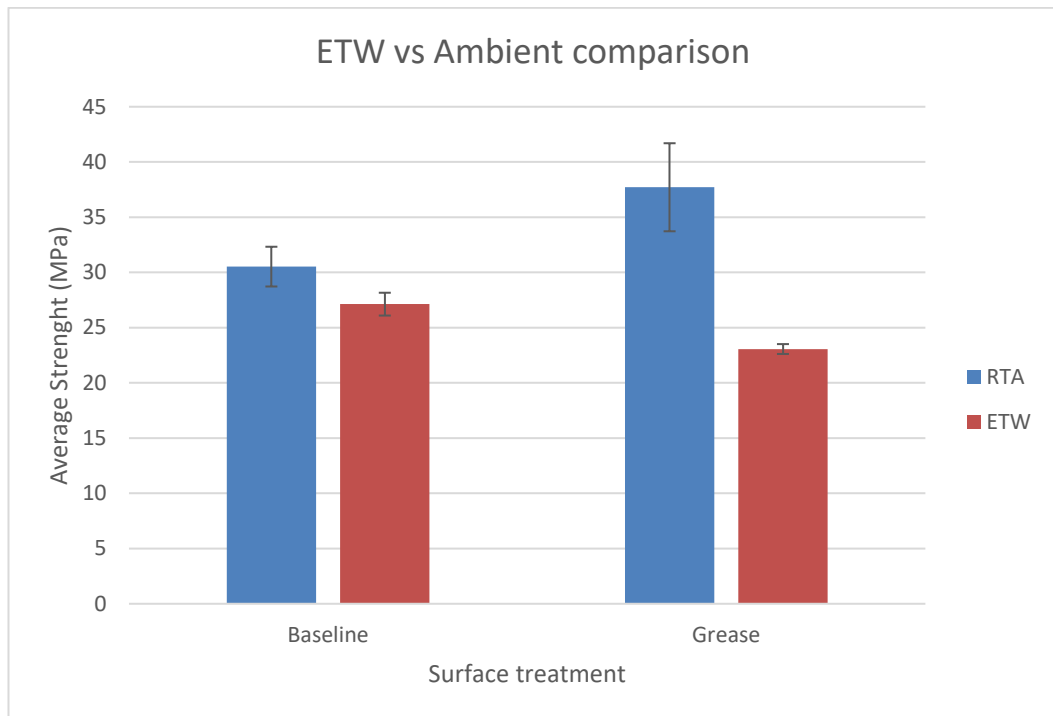


Figure 44: Comparison of the maximum average stress and SD between samples exposed to RTD and ETW environment

The exposure to the ETW environment reduced the strength of both types of samples, although the decrease was more substantial in the samples with grease contamination. Additionally, a decrease in the standard deviation of both types of samples is observed. This low SD could be explained by the quite-uniform failure surfaces of both Baseline ETW and Grease ETW samples. The failure surfaces of both RTA and ETW samples are presented in the following Figure 45, and in Figure 46 their average failure mode is plotted.



a) Baseline RTA (sample 3)



b) Baseline ETW (sample 4)



c) Grease RTA (sample 4)



d) Grease ETW (sample 3)

Figure 45: Comparison of RTA and ETW representative failure surfaces

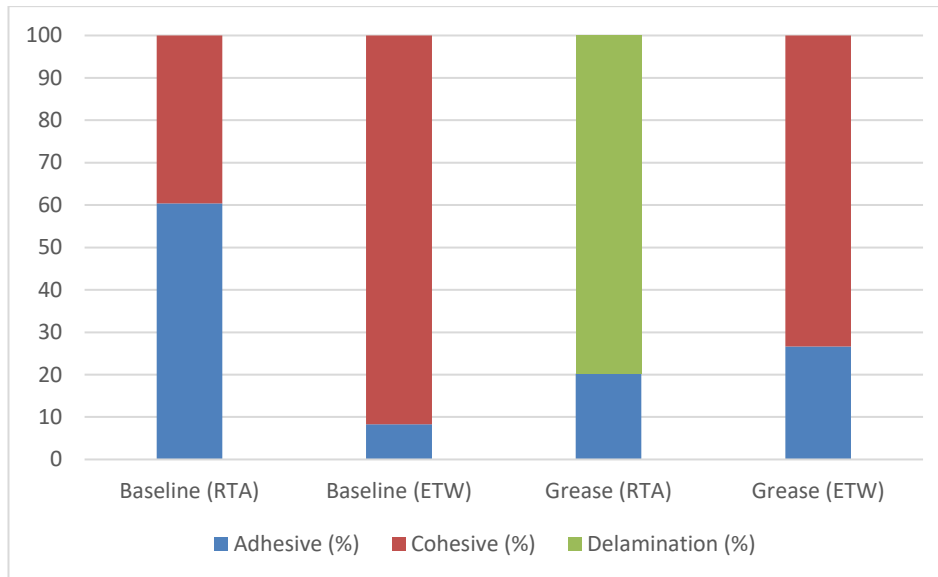


Figure 46: Average main failure mode in ETW samples compared with RTA counterparts

Unlike in RTA samples, the failure surfaces of Baseline ETW and Grease ETW look very similar, with a mainly cohesive failure complemented with some spots of adhesive failure. This is also reflected in Figure 46, where it can also be seen that Grease RTA had delamination as main failure mode, but after ETW conditioning there was no delamination failure: only cohesive and adhesive failure modes. Baseline ETW had a far higher cohesive failure presence than Baseline RTA, whose main failure mode was adhesive failure. Regarding the CA-strength correlation of ETW samples, Figure 47, 48 and 49 present the maximum average stress and the average, maximum and minimum contact angle, respectively, of both ETW and RTA Baseline and Grease samples. Additionally, linear trend lines are plotted for both RTA and ETW samples.

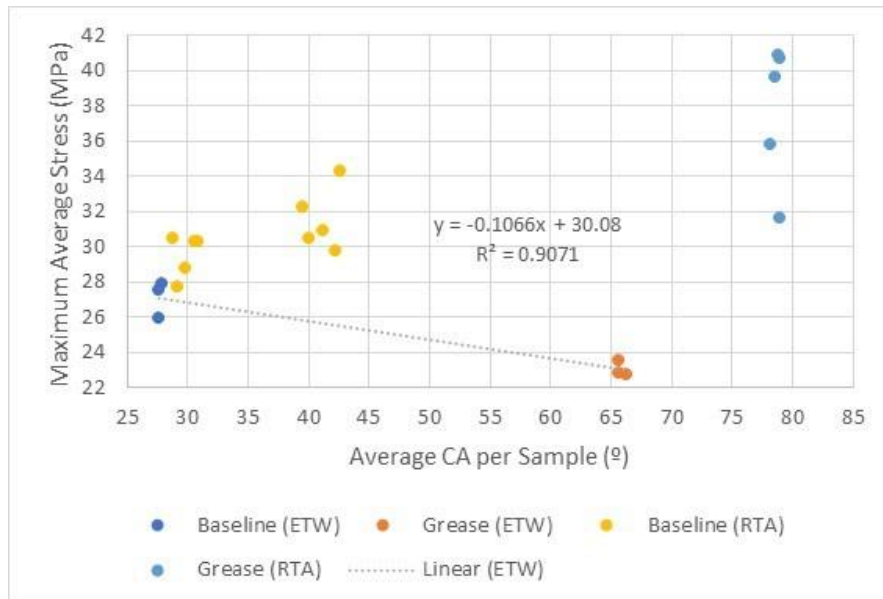


Figure 47: Joint strength – Average CA comparison of SLS ETW and RTA samples

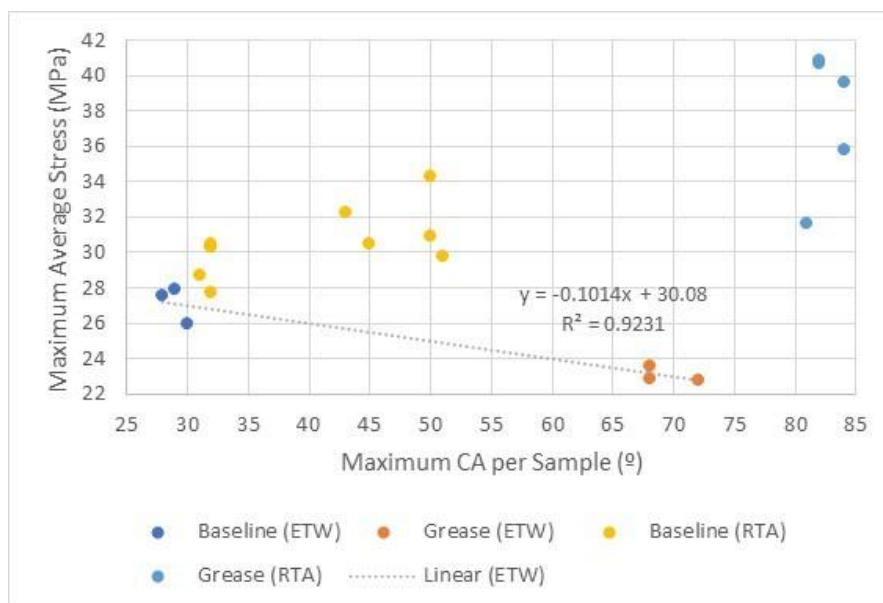


Figure 48: Joint strength – Maximum CA comparison of SLS ETW and RTA samples

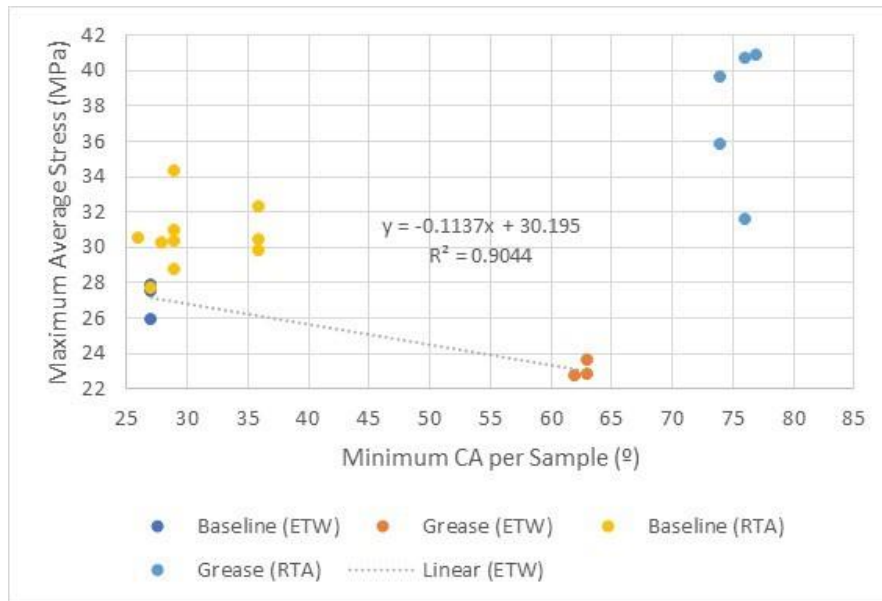


Figure 49: Joint strength – Minimum CA comparison of SLS ETW and RTA samples

Based on the graphs, a strong CA-strength correlation ($R^2 > 0.9$) is observed for the ETW samples: as the CA increases, the joint strength seems to deteriorate. This trend is observed with the average, the maximum and the minimum CA. Additionally, this trend could be related to the higher adhesive failure of Grease ETW samples when compared with Baseline ETW, as seen previously. On the other hand, the CA-strength correlation of RTA Baseline and Grease samples goes in the opposite direction: higher CA values seem to lead to higher joint strength. It should be noted that, unlike in previous subchapter 6.4, in this case only 2 surface treatments are being analysed for the RTA CA and strength data. Nevertheless, as already discussed when analysing all the RTA CA-strength results, the different failure modes of Baseline (adhesive and cohesive failure modes) and Grease (delamination and adhesive failure modes) could be the reason behind the strength difference and the CA-strength correlation obtained.

7. DISCUSSIONS

CA results discussion

Variations in contact angle values were observed between SLS and DSJ samples for the same surface treatment. This should not have happened, since both the surface treatments and the CA measurement procedure did not change from one type of sample to another. Nevertheless, some environmental factors such as temperature and RH were not controlled during the CA measurement process. This means that the room conditions were influenced by the external weather, and that could have affected the CA values measured. For example, this could explain the large standard deviation of SLS Baseline* samples, because half of the Baseline samples were manufactured in the summer of 2022 whereas the remaining half of Baseline samples and the whole Baseline ETW batch were manufactured in the spring of 2023. Moreover, since the CA measurements were performed in the laboratory where more researchers were working it is possible that there could be some dust on suspension in the air that could have deposited on the treated surface during the 15-minute dwell time between applying the surface treatment and measuring the CA. Other than environment-related factors, there are also numerous human-induced variations that could have affected the CA results. For example, variations in the sanding depth and pattern, which could have affected the surface roughness. This was probably the main reason the standard deviation of Light sanding samples was that high. Variations in the cleaning process (both with the dry-cloth and with MEK) as well as differences in the contamination process were also dependent on the operator, as well as the quantities used, even if the same procedure was followed each time. In the case of MEK4 treatment, the observed CA change could be due to the amount of MEK used during the cleaning process: some residual MEK could have remained in the surface significantly increasing the CA, and proving that MEK can be detected by measuring the CA.

In order to diminish the differences in CA values between SLS and DSJ samples 2 solutions are proposed:

1. Measuring the CA in a controlled environment, where the temperature and RH remain almost constant. Additionally, no dust-generating activities should be performed in the measuring environment.
2. Implanting automated sanding, cleaning and contamination processes. This would eliminate all human-induced variability factors in the results.

Based on the performed CA measurements with the different surface treatments and types of samples, measuring the surface contact angle proved an effective method to detect the presence of contaminants on carbon/epoxy laminates, even after cleaning them with a dry cloth, since the contact angle of contamination treatments ranged from 60 to 80°, whereas the average baseline CA was never exceeding 40°. It also detected consistently significant differences between various levels of sanding, which indicates that it is also able to detect changes in surface roughness in this type of laminates. Additionally, it could also detect whether a surface had been cleaned with MEK after sanding or not. Nevertheless, it had some problems differentiating a MEK cleaned surface from one contaminated with hydraulic fluid. Overall, these results prove the usefulness of contact angle measurement over other not-quantitative surface characterization techniques such as water break test, since the CA results are quantitative and can be interpreted more easily. Finally, in later research the CA measurements should be taken near the bonding area but outside of it, since the water drops deposited on the bonding surface could contaminate it and affect the resulting bond strength.

Strength results and failure surfaces discussion

The main observation that can be made from the testing results is that SLS and DSJ samples presented very different and contradictory tendencies, making it impossible to determine at first sight which are the best and the worst surface treatments to apply before bonding. Although the SLS testing is quite widespread due to its simplicity, SLS joints are known to experience substantial peel forces that should not be present in a pure shear test. Because of that, the results of DSJ are considered the most relevant ones, relegating the SLS results to a secondary role.

The surface treatments that resulted in the highest bond strength in DSJ were Baseline, Openlab contamination and Light sanding treatments. All of them have in common that no contaminant or cleaning agent is used after the surface roughening. On the other hand, MEK-cleaning and Grease, Jet fuel and Hydraulic fluid contamination treatments led to the lowest joint strength. Based on these DSJ results, cleaning the carbon fibre epoxy composite surface with MEK or contaminating it with hydraulic fluid resulted in the same result: a lower bond strength than just sanding and wiping the dust with a dry cloth. This is surprising, since MEK-cleaning is a common surface treatment of aircraft composites before bonding. Even if the SLS strength results were quite different from the ones of DSJ, this similarity between MEK-cleaning and contamination treatments was also observed, although in SLS MEK-cleaning and contamination treatments led to the highest strength. Because of that, more research is needed to confirm or to deny the results obtained in this thesis work.

Nevertheless, it should be noted that the strength results are not directly comparable, since the main failure mode was not the same in each surface treatment nor in each sample. The main failure modes in DSJ Baseline and Light sanding contaminated interfaces were adhesive and cohesive failure modes, although the batches with the highest strength (Baseline and Openlab) had delamination in a large part of their surfaces (>50%). On the other hand, in SLS samples delamination was the main failure mode of all but Baseline and Light sanding series, which had adhesive as main failure mode followed by cohesive failure mode. Naturally, these differences could have influenced the strength results of each sample, but determining and quantifying that influence is not an easy task. Moreover, identification of the main failure mode was not easy since adhesive failure of an epoxy adhesive with epoxy-matrix adherends is not as evident as the adhesive failure described in ASTM D5573, making the distinction between cohesive and adhesive failure modes hard to interpret visually.

Lastly, it should be noted that 82 out of all 84 RTA manufactured joints had a strength over the 25 MPa threshold commonly used in the industry to identify good bonding quality of FM 300-2 adhesive and also in some references like [45]. Additionally, it is uncertain how the different adhesive joints and surface treatments would have performed in a more service life-related mechanical test, such as a fatigue test. This and other long term strength degradation factors related to service life should be assessed in further research.

Contact angle – Bond strength correlation:

In DSJ a medium linear correlation ($R^2 = 0.7$) was observed for the minimum CA – strength results. The obtained correlation indicated that surface treatments with low surface CA resulted in adhesive joints with a high strength, whereas surface treatments with high CA values led to low bond strength. This trend was clearly visible for surface treatments with low CA and high bond strength, such as baseline sanding and open laboratory contamination, but also for high CA and low bond strength treatments like grease and jet fuel contamination. This trend is similar to the one obtained in both [24], [25] references, where the surfaces with the highest contamination and highest CA obtained the lowest bond strength. Nonetheless, the CA-strength correlation did not seem so clear in surface treatments providing medium CA values like MEK-cleaning, light sanding and hydraulic fluid contamination. To fully validate the obtained CA-strength correlation in DSJ it is necessary to study in more detail how the different failure modes influenced the bond strength and if there was a correlation between the measured CA and the main failure mode. For example, if there was a threshold CA value above or below which one

failure mode became the main one. Nevertheless, it should be noted that CA measurement only characterizes the properties of the adhesive-adherend interface, not the internal strength of the adhesive or the delamination strength of the adherend. Because of that, a clear CA-strength correlation could not be obtained from SLS data, since delamination was the main failure mode, resulting in a very low CA-strength linear correlation ($R^2 \approx 0.1$). Comparable results can be observed in [24], where samples with very similar CA obtained very different peel strength results due to differences in the main failure mode: samples that delaminated obtained significantly lower peel strength values than those that had mainly a cohesive failure mode.

Elevated temperature wet environment samples:

The obtained results were quite straightforward: ETW samples performed substantially worse than their RTA counterparts. This is in accordance with the traditionally accepted hypothesis that ETW environment exposition reduces the strength of adhesive joints in composites and it is also in accordance with the results of several papers like [31], [32]. Additionally, a quite strong CA-strength linear correlation was observed, with a coefficient of determination over 0.9, which indicated that low CA surfaces obtained higher bond strength, in accordance with some references like [26].

Regarding the main failure mode, a significant change was observed in both tested series. Both ETW series, baseline sanding and grease contamination, obtained a high cohesive failure mode (70-90%), but grease contamination and baseline sanding RTA treatments had delamination and adhesive failure as main failure modes, respectively.

It is interesting to note that the strength of the ETW samples was lower than RTA samples, but they had overall a lower adhesive failure. This could indicate that the adhesive-adherend interface did not degrade. On the other hand, the high cohesive failure and low joint strength could be related to the degradation of the internal strength of the FM 300-2 adhesive due to the ETW environment exposition.

Nevertheless, only 6 samples and 2 surface treatments were evaluated, which leaves plenty of room for further research. Additionally, a proper heated testing chamber should be used if available, although in this case it was not possible to do so.

8. CONCLUSIONS

Almost 100 adhesive joints of carbon fibre epoxy composites were manufactured and tested with the aim of determining the possible correlation between the contact angle of the laminate surface and the strength of the resulting adhesive joint, which was the main objective of this thesis. 8 different surface treatments were applied before bonding to SLS and DSJ samples to assess their influence in the surface CA values as well as in the adhesive joint strength, which could be considered as a secondary objective. Additionally, another secondary objective of the thesis was to study the effect of exposing adhesive joints with different surface treatments to a ETW environment and comparing the strength results to their RTA counterparts.

The main results of this thesis are the following:

- Contaminated and MEK-cleaned surfaces were easily differentiated from surfaces which had only been sanded by measuring the surface CA. Additionally, measuring the CA was also able to identify different surface roughening levels.
- The surface CA values measured with the same surface treatments were different in SLS and DSJ samples. Environmental conditions and human-induced process variations could be the reasons behind it.
- The strength results obtained with DSJ followed a different trend than SLS samples, observing also significant differences in the main failure modes. These differences could be a result of difference loading cases: DSJ loading is almost 100% shear, whereas in SLS testing there main loading is shear but there are also significant peel forces.
- Baseline sanding, open laboratory contamination and light sanding treatments resulted in the highest strength of DSJ, in that order. Nevertheless, these treatments led to different failure surfaces: open laboratory contamination and baseline sanding led to high delamination failure mode whereas light sanding resulted in a 90% adhesive failure mode. MEK-cleaning and other contamination processes significantly reduced the bonding strength of DSJ. Overall, the main failure mode of these treatments was a combination of adhesive, cohesive and delamination failure modes.
- On the other hand, MEK-cleaning and contamination surface treatments led to higher joint strengths than baseline and light sanding in SLS samples. The main

failure mode of the samples treated with MEK-cleaning and contamination treatments was delamination, with also a small contribution of adhesive failure. On the contrary, baseline and light sanding treatments resulted mainly in adhesive failure mode but also a significant cohesive failure mode.

- The strongest CA-strength correlation ($R^2 = 0.7$) observed in DSJ is the one between the minimum CA of each sample and its respective joint strength. The surface treatments that produced surfaces with low minimum CA resulted in adhesive joints with high bond strength, whereas contamination treatments with high surface CA led to low bond strength.
- The CA-strength correlation in SLS joints was inconclusive. This could be related to most of the samples experiencing delamination failures, but more research is needed to analyse its influence.
- The relationship between the surface CA, the failure mode and the joint strength of the tested samples needs to be studied more in detail. Further research should analyse, for example, if there is a threshold value above or below which one failure mode becomes dominant.
- Joints exposed to ETW environment had significantly lower strength than their RTA counterparts, even though their surface CA values before bonding very similar. Exposing the samples to ETW environment also changed the main failure mode of both tested surface treatments to cohesive failure. The strength of the adhesive could have degraded more than the adhesive-adherend interface.

REFERENCES

- [1] A. Hiken, 'The Evolution of the Composite Fuselage: A Manufacturing Perspective', in *Aerospace Engineering*, G. Dekoulis, Ed., IntechOpen, 2019. doi: 10.5772/intechopen.82353.
- [2] S. Karpuk, R. Radespiel, and A. Elham, 'Assessment of Future Airframe and Propulsion Technologies on Sustainability of Next-Generation Mid-Range Aircraft', *Aerospace*, vol. 9, no. 5, p. 279, May 2022, doi: 10.3390/aerospace9050279.
- [3] T. R. Brooks, G. Kennedy, and J. R. R. A. Martins, 'High-fidelity Multipoint Aerostructural Optimization of a High Aspect Ratio Tow-steered Composite Wing', in *58th AIAA/ASCE/AHS/ASC Structures, Structural Dynamics, and Materials Conference*, Grapevine, Texas: American Institute of Aeronautics and Astronautics, Jan. 2017. doi: 10.2514/6.2017-1350.
- [4] E. M. Greitzer *et al.*, 'N+3 Aircraft Concept Designs and Trade Studies, Final Report', *Final Rep.*, vol. 2, 2010.
- [5] E. Chesmar, *Care and repair of advanced composites*, 3rd ed. Warrendale, PA: SAE International, 2020.
- [6] M. C.-Y. Niu, *Composite airframe structures: practical design information and data*, 3rd ed. Hong Kong: Conmilit Press, 2010.
- [7] J. C. Gerdeen and R. A. L. Rorrer, *Engineering design with polymers and composites*, 2nd ed. Boca Raton, FL: CRC Press, 2012.
- [8] R. F. Gibson, *Principles of composite material mechanics*, Fourth edition. in *Mechanical engineering : a series of textbooks and reference books*. Boca Raton: CRC Press, Taylor & Francis Group, 2016.
- [9] X. Mi *et al.*, 'Toughness and its mechanisms in epoxy resins', *Prog. Mater. Sci.*, vol. 130, p. 100977, Oct. 2022, doi: 10.1016/j.pmatsci.2022.100977.
- [10] M. Bonmatin, F. Chabert, G. Bernhart, T. Cutard, and T. Djilali, 'Ultrasonic welding of CF/PEEK composites: Influence of welding parameters on interfacial temperature profiles and mechanical properties', *Compos. Part Appl. Sci. Manuf.*, vol. 162, p. 107074, Nov. 2022, doi: 10.1016/j.compositesa.2022.107074.
- [11] M. Thiruchitrabalam, D. Bubesh Kumar, D. Shanmugam, and M. Jawaid, 'A review on PEEK composites – Manufacturing methods, properties and applications', *Mater. Today Proc.*, vol. 33, pp. 1085–1092, Jan. 2020, doi: 10.1016/j.matpr.2020.07.124.
- [12] E. J. Barbero, *Introduction to composite materials design*, Third edition. in *Composite materials : analysis and design*. Boca Raton: CRC Press, Taylor & Francis Group, CRC Press is an imprint of the Taylor & Francis Group, an informa business, 2018.
- [13] F. C. Campbell, *Manufacturing processes for advanced composites*. New York: Elsevier, 2004.
- [14] Ch. V. Katsiropoulos, A. N. Chamos, K. I. Tserpes, and Sp. G. Pantelakis, 'Fracture toughness and shear behavior of composite bonded joints based on a novel aerospace adhesive', *Compos. Part B Eng.*, vol. 43, no. 2, pp. 240–248, Mar. 2012, doi: 10.1016/j.compositesb.2011.07.010.
- [15] S. Ebnesajjad and C. F. Ebnesajjad, *Surface treatment of materials for adhesive bonding*, Second edition. Amsterdam: William Andrew, an imprint of Elsevier, 2014.
- [16] S. Wu, *Polymer Interface and Adhesion*, 1st ed. Routledge, 2017. doi: 10.1201/9780203742860.
- [17] D14 Committee, 'Terminology of Adhesives', ASTM International. doi: 10.1520/D0907-12.
- [18] C. A. Harper, Ed., *Handbook of plastics, elastomers, and composites*, 4th ed. in *McGraw-Hill handbooks*. New York: McGraw-Hill, 2002.

- [19] W. Wang, J. A. Poulis, S. T. D. Freitas, and D. Zarouchas, 'SURFACE PRETREATMENTS ON CFRP AND TITANIUM FOR MANUFACTURING ADHESIVELY BONDED BI-MATERIAL JOINTS', 2018.
- [20] 'DIN EN ISO 9000:2015-11, Qualitätsmanagementsysteme_ Grundlagen und Begriffe (ISO_9000:2015); Deutsche und Englische Fassung EN_ISO_9000:2015', Beuth Verlag GmbH. doi: 10.31030/2325650.
- [21] 'DIN 2304-1:2016-03, Klebtechnik_ Qualitätsanforderungen an Klebprozesse_ Teil_1: Prozesskette Kleben', Beuth Verlag GmbH. doi: 10.31030/2399371.
- [22] R. C. Snogren, *Handbook of Surface Preparation*. NY: Palmerton Publishing Co., 1974.
- [23] A. Bechikh, O. Klinkova, Y. Maalej, I. Tawfiq, and R. Nasri, 'Effect of dry abrasion treatments on composite surface quality and bonded joints shear strength', *Int. J. Adhes. Adhes.*, vol. 113, p. 103058, Mar. 2022, doi: 10.1016/j.ijadhadh.2021.103058.
- [24] A. R. G, B. S. W, and H. Pascal, 'Effect of Varying Levels of Peel Ply Contamination on Adhesion Threshold', in *SAMPE 2010 - New Materials and Processes for a New Economy, Seattle WA, May 17–20, 2010*, Society for the Advancement of Material and Process Engineering (SAMPE), 2010, pp. 1–1.
- [25] C. Dighton, A. Rezai, S. L. Ogini, and J. F. Watts, 'Atmospheric plasma treatment of CFRP composites to enhance structural bonding investigated using surface analytical techniques', *Int. J. Adhes. Adhes.*, vol. 91, pp. 142–149, Jun. 2019, doi: 10.1016/j.ijadhadh.2019.03.010.
- [26] C. Sun, J. Min, J. Lin, H. Wan, S. Yang, and S. Wang, 'The effect of laser ablation treatment on the chemistry, morphology and bonding strength of CFRP joints', *Int. J. Adhes. Adhes.*, vol. 84, pp. 325–334, 2018, doi: <https://doi.org/10.1016/j.ijadhadh.2018.04.014>.
- [27] G. Yang, T. Yang, W. Yuan, and Y. Du, 'The influence of surface treatment on the tensile properties of carbon fiber-reinforced epoxy composites-bonded joints', *Compos. Part B Eng.*, vol. 160, pp. 446–456, Mar. 2019, doi: 10.1016/j.compositesb.2018.12.095.
- [28] E. Akman, Y. Erdoğan, M. Ö. Bora, O. Çoban, B. G. Oztoprak, and A. Demir, 'Investigation of accumulated laser fluence and bondline thickness effects on adhesive joint performance of CFRP composites', *Int. J. Adhes. Adhes.*, vol. 89, pp. 109–116, 2019, doi: <https://doi.org/10.1016/j.ijadhadh.2018.12.003>.
- [29] B. D. Flinn, B. K. Clark, J. Satterwhite, and P. J. Van Voast, 'Influence of peel ply type on adhesive bonding of composites', in *International SAMPE Symposium and Exhibition (Proceedings)*, 2007.
- [30] Sp. Pantelakis and K. I. Tserpes, 'Adhesive bonding of composite aircraft structures: Challenges and recent developments', *Sci. China Phys. Mech. Astron.*, vol. 57, no. 1, pp. 2–11, Jan. 2014, doi: 10.1007/s11433-013-5274-3.
- [31] G. A. Knight, T. H. Hou, M. A. Belcher, F. L. Palmieri, C. J. Wohl, and J. W. Connell, 'Hygrothermal aging of composite single lap shear specimens comprised of AF-555M adhesive and T800H/3900-2 adherends', *Int. J. Adhes. Adhes.*, vol. 39, pp. 1–7, Dec. 2012, doi: 10.1016/j.ijadhadh.2012.06.009.
- [32] S. Liu, X. Cheng, Q. Zhang, J. Zhang, J. Bao, and X. Guo, 'An investigation of hygrothermal effects on adhesive materials and double lap shear joints of CFRP composite laminates', *Compos. Part B Eng.*, vol. 91, pp. 431–440, Apr. 2016, doi: 10.1016/j.compositesb.2016.01.051.
- [33] F. Zhang, H.-P. Wang, C. Hicks, X. Yang, B. E. Carlson, and Q. Zhou, 'Experimental study of initial strengths and hygrothermal degradation of adhesive joints between thin aluminum and steel substrates', *Int. J. Adhes. Adhes.*, vol. 43, pp. 14–25, Jun. 2013, doi: 10.1016/j.ijadhadh.2013.01.001.
- [34] Y.-B. Park, M.-G. Song, J.-J. Kim, J.-H. Kweon, and J.-H. Choi, 'Strength of carbon/epoxy composite single-lap bonded joints in various environmental conditions',

- Compos. Struct.*, vol. 92, no. 9, pp. 2173–2180, Aug. 2010, doi: 10.1016/j.compstruct.2009.09.009.
- [35] W. L. Cavalcanti, K. Brune, M. Noeske, K. Tserpes, W. M. Ostachowicz, and M. Schlag, Eds., *Adhesive bonding of aircraft composite structures: non-destructive testing and quality assurance concepts*. Cham: Springer, 2021.
- [36] A. Benatar, 'Plastics Joining', in *Applied Plastics Engineering Handbook*, Elsevier, 2017, pp. 575–591. doi: 10.1016/B978-0-323-39040-8.00027-4.
- [37] K. L. Mittal, S. K. Panigrahi, and John Wiley & Sons, Inc, Eds., *Structural adhesive joints: design, analysis and testing*. Hoboken, NJ: Wiley-Scrivener, 2020.
- [38] 'Standard Test Method for Lap Shear Adhesion for Fiber Reinforced Plastic (FRP) Bonding'. <https://www.astm.org/d5868-01r14.html> (accessed Jun. 22, 2023).
- [39] 'Standard Test Method for Strength Properties of Double Lap Shear Adhesive Joints by Tension Loading'. <https://www.astm.org/d3528-96r16.html> (accessed Jun. 22, 2023).
- [40] L. J. Hart-Smith, 'Adhesively Bonded Joints in Aircraft Structures', in *Handbook of Adhesion Technology*, L. F. M. Da Silva, A. Öchsner, and R. D. Adams, Eds., Berlin, Heidelberg: Springer Berlin Heidelberg, 2011, pp. 1101–1147. doi: 10.1007/978-3-642-01169-6_44.
- [41] R. D. Adams, Ed., *Adhesive bonding: science, technology and applications*. Boca Raton : Cambridge: CRC Press ; Woodhead Pub, 2005.
- [42] D14 Committee, 'Practice for Classifying Failure Modes in Fiber-Reinforced-Plastic (FRP) Joints', ASTM International. doi: 10.1520/D5573-99R19.
- [43] S. Ebnesajjad and A. H. Landrock, 'Adhesives Technology Handbook (3rd Edition)', [Online]. Available: <https://app.knovel.com/hotlink/toc/id:kpATHE0004/adhesives-technology/adhesives-technology>
- [44] Cyttec Engineered Materials, 'FM 300-2 Film Adhesive Technical Data Sheet'. https://www.pccomposites.com/wp-content/uploads/2015/07/PCA250-2M06_TDS.pdf (accessed Jun. 20, 2023).
- [45] J. Aakkula, O. Saarela, T. Haikola, and S. Tervakangas, 'DIARC plasma coating for reliable and durable structural bonding of metals', in *28th International Congress of the Aeronautical Sciences, Brisbane Australia, 23-28 September 2012*, Optimage Ltd, 2012. Accessed: Jun. 21, 2023. [Online]. Available: <https://research.aalto.fi/en/publications/diarc-plasma-coating-for-reliable-and-durable-structural-bonding->

APPENDIX A: CONTACT ANGLE DATA

This appendix contains data about the contact angle measurements performed to each type of sample and surface treatment.

Table A 1: Contact angle data of SLS samples

Surface treatment	Average CA (°)	Max. CA (°)	Min. CA (°)	SD (°)
Baseline	36	51	26	7
Baseline (ETW)	28	30	26	1
Baseline*	33	51	26	7
Light sanding	46	67	33	9
Openlab	33	35	31	1
MEK1	63	69	54	4
MEK4	46	54	37	5
Jet fuel	74	81	70	3
Hydraulic fluid	71	78	63	4
Grease	79	84	74	2
Grease (ETW)	66	72	61	2
Grease*	72	84	61	7

Table A 2: Contact angle data of contaminated DSJ interfaces

Surface treatment	Average CA (°)	Max. CA (°)	Min. CA (°)	SD (°)
Baseline	40	52	32	5
Light sanding	64	83	38	10
Openlab	38	43	34	2
MEK1	58	63	53	3
MEK4	62	67	55	4
Jet fuel	69	72	66	2
Hydraulic fluid	59	62	56	2
Grease	74	79	68	3

Table A 3: Comparison of SLS and DSJ contact angle data

Surface treatment	SLS CA (Avg. \pm SD)	DSJ CA (Avg. \pm SD)
Baseline*	33 \pm 7	40 \pm 5
Light sanding	46 \pm 9	64 \pm 10
Openlab	33 \pm 1	38 \pm 2
MEK1	63 \pm 4	58 \pm 3
MEK4	46 \pm 5	62 \pm 4
Jet fuel	74 \pm 3	69 \pm 2
Hydraulic fluid	71 \pm 4	59 \pm 2
Grease*	72 \pm 7	74 \pm 3

APPENDIX B: MECHANICAL TESTING DATA

In this appendix the force and strength results of each sample are presented, as well as each sample bonding width used to calculate their stress.

Table B 1: Maximum force of each SLS sample during testing

	Maximum force (kN) in SLS samples				
	Sample number				
Surface treatment	1 (6)	1 (6)	1 (6)	1 (6)	1 (6)
Baseline (1-5)	9.64	11.06	9.98	10.37	9.83
Baseline (6-10)	9.74	9.74	9.28	8.92	9.80
Light	9.80	9.23	9.32	8.72	9.03
Openlab	12.70	14.90	13.75	14.93	14.86
MEK1	14.43	16.22	16.30	14.76	15.19
MEK4	16.04	14.76	15.45	15.02	14.77
Jet fuel	15.31	14.96	15.21	14.67	13.19
Hydraulic fluid	15.42	14.87	14.46	14.21	13.83
Grease	12.82	11.59	13.19	13.25	10.24
Baseline (ETW)	8.41	9.02	8.88		
Grease (ETW)	7.58	7.37	7.33		

Table B 2: Maximum force of each DSJ sample during testing

	Maximum force (kN)				
	Sample number				
Surface treatment	1	2	3	4	5
Baseline	27.51	28.83	26.57	22.67	22.80
Light	25.00	20.86	24.83	25.48	
Openlab	19.15	25.37	26.70	26.99	26.05
MEK1	16.16	19.65	18.95	17.66	17.25
MEK4	17.02	18.01	18.78	18.52	18.48
Jet fuel	19.28	17.75	18.42	17.67	17.71
Hydraulic fluid	19.41	18.94	20.57	20.84	18.41
Grease	15.87	16.03	16.21	16.60	18.63

Table B 3: Bonding width of each SLS sample

	Bonding width (mm)				
	Sample number				
Surface treatment	1 (6)	2 (7)	3 (8)	4 (9)	5 (10)
Baseline (1-5)	25.47	25.39	25.39	25.32	25.41
Baseline (6-10)	25.32	25.29	25.41	25.36	25.32
Light	25.3	25.32	25.36	25.31	25.33
Openlab	24.91	25.83	24.04	24.81	24.85
MEK1	25.42	25.38	25.37	25.49	25.46
MEK4	25.5	25.5	25.47	25.47	25.52
Jet fuel	25.41	25.36	25.38	25.42	25.48
Hydraulic fluid	25.49	25.5	25.42	25.62	25.53
Grease	25.48	25.54	25.5	25.54	25.55
Baseline (ETW)	25.51	25.48	25.4		
Grease (ETW)	25.31	25.4	25.35		

Table B 4: Bonding width of each DSJ sample

	Bonding width (mm)				
	Sample number				
Surface treatment	1	2	3	4	5
Baseline	25.37	25.38	25.34	25.09	25.34
Light	25.33	25.28	25.26	25.37	
Openlab	25.22	25.19	25.26	25.27	25.27
MEK1	26.08	25.35	25.28	25.23	25.28
MEK4	25.37	25.37	25.40	25.36	25.32
Jet fuel	25.30	25.33	25.35	25.29	25.48
Hydraulic fluid	25.28	25.36	25.25	25.21	25.21
Grease	25.21	25.18	25.27	25.54	25.61

Table B 5: Maximum stress of each SLS sample during testing

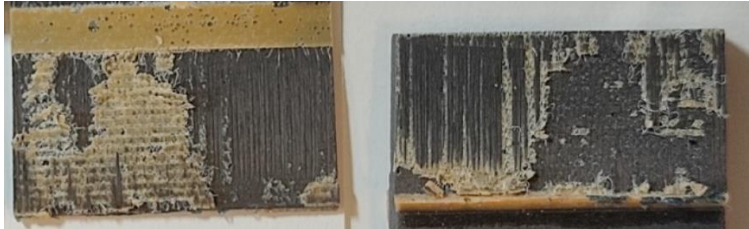
	Maximum stress (MPa)				
	Sample number				
Surface treatment	1 (6)	2 (7)	3 (8)	4 (9)	5 (10)
Baseline (1-5)	29.80	34.29	30.94	32.25	30.46
Baseline (6-10)	30.28	30.32	28.74	27.69	30.48
Light	30.51	28.70	28.95	27.13	28.08
Openlab	40.14	45.42	45.03	47.40	47.08
MEK1	44.69	50.32	50.58	45.60	46.97
MEK4	49.53	45.58	47.77	46.44	45.57
Jet fuel	47.43	46.45	47.18	45.44	40.75
Hydraulic fluid	47.66	45.86	44.66	43.82	42.62
Grease	39.61	35.79	40.84	40.71	31.59
Baseline (ETW)	25.95	27.89	27.54		
Grease (ETW)	23.58	22.85	22.77		

Table B 6: Maximum stress of each DSJ sample during testing

	Maximum stress (MPa)				
	Sample number				
Surface treatment	1	2	3	4	5
Baseline	42.69	44.73	41.28	35.58	35.41
Light	38.86	32.48	38.70	39.53	
Openlab	29.89	39.65	41.63	42.04	40.58
MEK1	24.40	30.52	29.50	27.56	26.87
MEK4	26.41	27.95	29.11	28.75	28.74
Jet fuel	30.01	27.59	28.61	27.51	27.36
Hydraulic fluid	30.22	29.41	32.08	32.54	28.74
Grease	24.79	25.07	25.25	25.60	28.64

APPENDIX C: FAILURE SURFACES IMAGES

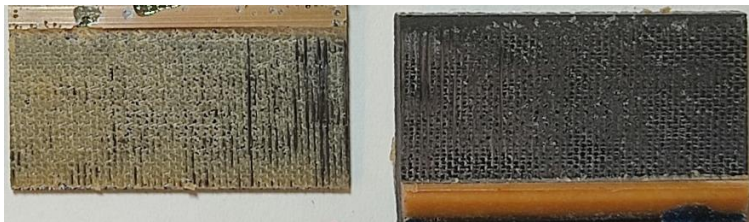
This appendix presents pictures of contaminated (C) and non-contaminated (NC) DSJ failure interfaces for each surface treatment.



Baseline

Sample 4

Interface E&F



Light

Sample 3

Interface E&F



Openlab

Sample 2

Interface C&D



MEK1-C

Sample 4

Interface G&H



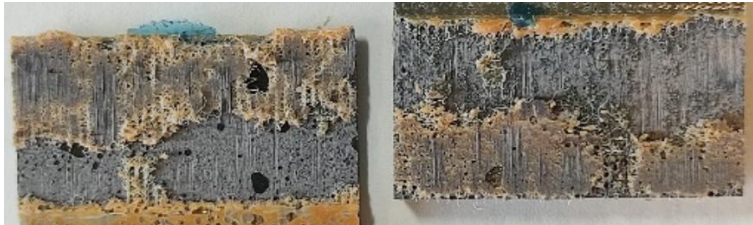
MEK1-NC

Sample 4

Interface C&D



MEK4-C
Sample 2
Interface G&H



MEK4-NC
Sample 4
Interface C&D



Jet fuel-C
Sample 4
Interface E&F



Jet fuel-NC
Sample 1
Interface C&D



Hydraulic fluid-C
Sample 4
Interface G&H



Hydraulic fluid-NC
Sample 3
Interface C&D



Grease-C
Sample 3
Interface G&H



Grease-NC
Sample 2
Interface A&B

Figure C 1: Representative images of contaminated and non-contaminated DSJ failure surfaces for each surface treatment